THESIS FOR THE DEGREE OF DOCTOR OF PHILOSOPHY

Specific ion effects in carboxymethyl cellulose adsorption on cellulose:
A step towards modification of fibers in fiber line

VISHNU ARUMUGHAN

Department of Chemistry and Chemical Engineering

CHALMERS UNIVERSITY OF TECHNOLOGY

Gothenburg, Sweden 2022

Specific ion effects in carboxymethyl cellulose adsorption on cellulose: A step towards modification of fibers in fiber line

VISHNU ARUMUGHAN
ISBN 978-91-7905-616-2

Doktorsavhandlingar vid Chalmers tekniska högskola
Ny serie nr 4901
ISSN0346-718X

Department of Chemistry and Chemical Engineering
Chalmers University of Technology
SE-412 96 Gothenburg
Sweden
Telephone + 46 (0)31-772 1000

I, Vishnu Arumughan, hereby certify that this thesis is my original work and, to the best of my knowledge, does not contain any material previously published or written by another person, except where due reference or acknowledgement is made.

Cover: The image depicts the adsorption of CMC chains (green) on the surface of cellulose in the presence of calcium ions (orange)

Printed by:
Chalmers digitaltryck
Gothenburg, Sweden 2022

I dedicate this thesis to my beloved parents

Specific ion effects in carboxymethyl cellulose adsorption on cellulose:

A step towards the modification of fibers in fiber line

Vishnu Arumughan
Department of Chemistry and Chemical Engineering
Chalmers University of Technology

Abstract

The increasing global demands for paper products have fuelled the research in developing new fibers from existing industrial processes. The adsorption of carboxymethyl cellulose (CMC) has been shown to improve the tensile properties of the paper significantly. One way to manufacture such modified fibers is to integrate the CMC adsorption step in current pulping mills. However, the mechanism behind the adsorption of CMC on cellulose surfaces is still not fully understood, even if the literature on this subject is extensive. This thesis discusses the controlling factors and mechanism behind the adsorption of CMC on cellulose surfaces, which can enable future integration of adsorption process within the pulping mill.

The adsorption studies have been carried out mainly on model cellulose surfaces using QCM-D and it was shown that the CMC absorption depends on the amount and type of added cations and anions. The ion specificity in CMC adsorption was explained by these ions' ability to induce dispersion forces and hydration regulated positioning of ions at the interface. The observation that CMC adsorption on the model system is ion-specific was confirmed in a study where CMC was absorbed on commercially available softwood kraft pulp. Furthermore, CMC adsorption on cellulose model surfaces in the presence of D_2O or H_2O revealed that this process is entropy driven, which was supported by temperature dependent adsorption experiments.

Keywords: Polymer adsorption, Cellulose, Carboxymethyl cellulose, Specific ionic effects

List of Articles

This thesis is based on the work contained in the following articles:

1. **Fundamental aspects of the non-covalent modification of cellulose via polymer adsorption**
   Arumughan, V., Nypelö, T., Hasani, M. and Larsson, A., *Advances in Colloids and Interface Science,* **2021,** *298*, 102529. (Review)

2. **Specific ion effects in the adsorption of carboxymethyl cellulose: the influence of industrially relevant divalent cations**
   Arumughan, V., Nypelö, T., Hasani, M., Brelid, H., Albertsson, S., Wågberg, L. and Larsson, A., *Colloids and Surfaces A: Physicochemical and Engineering Aspects*, **2021,** *626*, 127006.

3. **Calcium ion induced structural changes in carboxymethyl cellulose solution and their effect on adsorption on cellulose surfaces**
   Arumughan, V., Nypelö, T., Hasani, M. and Larsson, A. *Biomacromolecules*, **2022**, *23*, 47.

4. **Anion specific adsorption of carboxymethyl cellulose on cellulose**
   Arumughan, V., Örzen, H., Hedenqvist, M**.,** M. Skepö, Nypelö, T., Hasani, M., and Larsson, A., **2022** (Manuscript).

Contribution Report

1. Conceived the idea for the review with the guidance of A.L and wrote the draft with inputs from T.N and M.H.

2. Conceived the idea for the project with A.L and performed all experiments, except the surface charge analysis, and wrote the manuscript with inputs from all co-authors

3. Conceived the idea for the project with A.L and performed all experiments and wrote the manuscript. The final editing of the manuscript was carried out by A.L, T.N and M.H

4. Conceived the idea for the project with A.L and performed all the experiments except molecular dynamic simulations. VA wrote the manuscript with inputs from H.O.

Additionally, this thesis contains unpublished data that were not included in any of the above-mentioned manuscripts. Following the figure captions, the credits have been referenced.

Publications not included in this thesis

1. **Nanocellulose-based membranes for water purification**
   Gopakumar, D.A., Arumughan, V., Pasquini, D., Leu, S.Y.B., HPS, A.K. and Thomas, S., In *Nanoscale Materials in Water Purification* **2019,** 59. Elsevier.

2. **Nanolignocellulose extracted from environmentally undesired Prosopis juliflora**
   Valencia, L., Arumughan, V., Jalvo, B., Maria, H.J., Thomas, S. and Mathew, A.P., *ACS Omega*, **2019**, *4,* 4330.

3. **Robust superhydrophobic cellulose nanofiber aerogel for multifunctional environmental applications**
   Gopakumar, D.A., Arumughan, V., Pottathara, Y.B., KS, S., Pasquini, D., Bračič, M., Seantier, B., Nzihou, A., Thomas, S., Rizal, S. and Khalil HPS., *Polymers*, **2019**, *11*, 495.

4. **Carbon dioxide plasma treated PVDF electrospun membrane for the removal of crystal violet dyes and iron oxide nanoparticles from water**
   Gopakumar, D.A., Arumughan, V., Gelamo, R.V., Pasquini, D., de Morais, L.C., Rizal, S., Hermawan, D., Nzihou, A. and Khalil, H.A., *Nano-Structures & Nano-Objects*, **2019,** *18*, 100268.

5. **Mechanically Robust Antibacterial Nanopapers Through Mixed Dimensional Assembly for Anionic Dye Removal**
   Nizam, P.A., Arumughan, V., Baby, A., Sunil, M.A., Pasquini, D., Nzihou, A., Thomas, S. and Gopakumar, D.A. *Journal of Polymers and the Environment*, **2020**, *28*, 1279.

6. **Prototype Gastro-Resistant Soft Gelatin Films and Capsules—Imaging and Performance In Vitro**
   Maciejewski, B., Arumughan, V., Larsson, A. and Sznitowska, M., *Materials*, **2020,** *13*,1771.

7. **N_2O assisted siphon-foaming of modified galactoglucomannans with cellulose nanofibrils**
   Nypelö, T., Fredriksson, J., Arumughan, V., Larsson, E., Hall, S.A. and Larsson, A. *Frontiers in Chemical Engineering*, **2021,** *3*, 756026.

Acknowledgements

First of all, I would like to acknowledge Södra Skogsägarna ekonomisk förening, Södra Foundation for Research, Development and Education and Treesearch, for funding my research. Treesearch has funded this research through the strategic innovation program BioInnovation, a joint venture between Vinnova, Formas and the Swedish Energy Agency.

The past four years have been the most exciting and eventful period of my life. There are a number of people that I must acknowledge for making my PhD journey exciting and even possible. To begin, I would like to express my heartfelt gratitude to my main supervisor, Prof. Anette Larsson, for giving me the opportunity to pursue my PhD under her guidance. You are the best supervisor a person could wish for. Your prompt guidance and the freedom you gave to me to follow my own ideas were priceless and had a vital influence in shaping me as a researcher. You have also had a personal impact on me; I believe that throughout the course of four years of frequent interaction with you, you have instilled in me a positive attitude and compassion. Along with all these wonderful things, you also managed to pass on to me your love for Cola Zero. However, when I consider the nice things you've given me, I see that quitting a bad habit is manageable. Once again, many thanks.

I would like to express my gratitude to my co-supervisors, Sverker Albertsson (late), Dr. Merima Hasani, and Dr. Fredrik Wernersson Brodin, for their unwavering support and encouragement.

I would like to express my deepest thanks to Dr. Tiina Nypelö for showing me the ropes on QCM-D and AFM and also providing constructive input on my manuscripts. I would also like to express thanks for providing me with the opportunity to read and discuss 'Polymers at Interface' with my peers. That book was truly transformative. At this point, I would want to express my gratitude to Gain, Justas, John, and Gustav for the discussions we had throughout the course.

I would like to express my gratitude to all Staffs at Södra Innovation, especially Harald Brelid for sharing his expertise and giving me proper direction in research during my visit to Södra Innovation.

I would also like to thank everyone involved in AvanCell 4. Especially, Axel Martinsson, Hans Theliander, Sven Hermansson, and Espen Ribe.

I would like to thank all my collaborators, particularly Prof. Ali Assifoui (University of Burgundy) for the ITC measurements and, more importantly, for the interesting discussions we had about cinema and science during your stay at Chalmers. I would like to express my deepest gratitude to Prof. Lars Wågberg (KTH) for his constructive feedbacks on my second article; Marie Skepö (Lund) for her suggestions in experimental design in article 4; Hüsamettin D Özeren and Mikael Hedenqvist for agreeing to help me with simulations for article 4.

A very special thanks to past and present members of Larsson/Nypelö/Strom groups. The way we work in our groups is something unique, at least, I have not seen such cooperation in any other places. Anna, Anette and Tiina thanks for your collective effort to make such environment. Robin, Roujin, Pegah, Rydvikha, Saul, Gain, Ehsan, Åke, Elliot, Jakob, Leo, Bahiru, Panos, Patricia, Aline - Thank you very much for being the best group mates and office mates.

I would like to thank Prof. Christian Muller for his role as my examiner and Prof. Lars Evenäs for being the best director of studies of Material science graduate school.

I would like to thank Lotta Petersson for the help with administrative things and making applied chemistry a great workplace with lot of fun activities.

I would also like express a special thanks to Eric, Nizam, Roujin and Akshay for proof correcting the thesis.

Being thousand miles away from home was a tough task, especially for someone with severe home sickness like me. I thank my friends, Siriyac, Vineeth, Arun, Ashwin, Shyam, Doyel, Sourav, Akshay for being there for me.

To my beloved parents Arumughan and Sulatha. Thanks for shaping me to what I am today and providing all the support and love. There were times during the four years when you needed my presence as a son and I wasn't able to physically be there for you, but you managed to get by without me, I thank my brother Pranav for covering for me.

Last but not least my wife Amritha, thanks for being there for me in all up and downs and also for helping me choosing right colour schemes in figures. Anette once told me, after you moved in, I became very productive. Definitely, your presence had a positive impact in finishing this thesis earlier than expected.

Abbreviations

AFM	Atomic force microscopy
APTES	Aminopropyltriethylsilane
CMC	Carboxymethyl cellulose
CNC	Cellulose nanocrystals
CNF	Cellulose nanofibers
DLS	Dynamic light scattering
DS	Degree of substitution
ECF	Elemental chlorine free
EDL	Electrical double layer
IEP	Isoelectric points
IHP	Inner Helmholtz plane
ITC	Isothermal Titration Calorimetry
LB	Langmuir-Blodgett
LMWA	Law of match making water affinities
NMNO	N-methylmorpholine N-oxide
OHP	Outer Helmholtz plane
PEDOT: PSS	Poly(3,4-ethylenedioxythiophene) polystyrene sulfonate
PEI	Polyethyleneimine
PSD	Particle size distribution
QCM-D	Quartz crystal microbalance
Rh	Hydrodynamic radius
SF-Theory	Scheutjens-Fleer polymer adsorption theory
SPAR	Stagnation point adsorption reflectometry
SPR	Surface plasmon resonance
TCF	Total chlorine free
TEMPO	(2,2,6,6-Tetramethylpiperidin-1-yl)oxyl
TFA	Trifluoroaceticacid
TMSC	Trimethylsilyl cellulose
TOC	Total organic carbon

Table of contents

Chapter 1

Introduction

Trees have played a significant role in the emergence of humanity as a developed social species. All our technological progress may be traced back to the invention of fire and the wheel. Historical documents suggest that wood was instrumental in these discoveries[1,2]. Throughout the ancient Indian subcontinent and Southeast Asia, palm leaves were used to write texts from literary masterpieces to scientific astronomy and mathematics[3]. A writing surface made of a paper-like material produced from Cyperus papyrus was used in ancient Egypt[4]. Documented evidence indicates China was the birthplace of the first paper production process, which was later adopted to the Middle East, and then to Europe by the 11th century. Later in Europe, wood-based paper processing was invented[5]. This was a big step forward in the papermaking process. From that point, both paper and paper-based industries had markable involvement in the development of our society.

Coming to the modern era, digitalization is a new reality that drastically changed our daily lives. Due to the digitalization, the demand for conventional paper products has decreased significantly. However, demand for paper goods such as tissue papers and packaging materials has surged because of consumer behaviour shifts and the introduction of online shopping services[6]. In addition, governmental policies and awareness about climate changes also contributed to the demands for paper products such as packaging materials.

The growing demand for specialized paper products has compelled businesses to reimagine their existing industrial processes to create new fibers with novel functions that will enable them to remain profitable. A competitive and lucrative forest sector may pioneer new processes, products, materials, and services, all of which contribute to social growth on a sustainable basis[7]. However, it is critical to continuously improve existing processes and products for an industry to remain competitive. This aspect was stressed in Sweden's forest industries' Research Agenda 4.0[7]. Over the years, the forest industry has gone through several improvements in the production and processing of cellulose pulps. The main focus of process optimization was to reduce water consumption and energy usage in production, resulting in a considerable increase in resource efficiency. The efforts are continuing in this regard.

The development of new pulp and fiber qualities and the modification of cellulose are the basis for the development of new fiber-based products. This also includes

the need to develop process stages and integrated process solutions for new products[7]. Both chemical and physical methods can achieve the modification of cellulose fibers. Chemical modification of cellulose often entails converting hydroxyl groups on the fiber surface into ethers, esters, acids, and so on[8]. Additionally, diverse functional groups can be incorporated into the fiber surface by non-covalent adsorption of various functional polymers[9]. Polymer adsorption has been used in the paper industry for a long time. One of the major examples is the recirculation of xylan for increasing the carbohydrate yield, the primary mechanism at play in this is the re-adsorption of xylans back to the fiber surface. Different synthetic polymers have also been used in the paper industry to improve the physical properties of paper[10].

Numerous attempts have been made earlier to explore the adsorption of various polymers on cellulose surfaces in order to gain a better understanding of the process at the molecular level[10]. One could wonder how understanding the process at the molecular level will help to solve industrial challenges. However, I feel that a better understanding of the mechanism and governing factors would allow for more precise tuning of the process. Recently, interest in combining polymer adsorption with existing pulp mills has increased, allowing for resource-efficient modification of cellulose fibers during the manufacturing process[11]. A thorough understanding of the polymer adsorption process can aid in the development of innovative procedures for fiber modification that take use of the conditions present during kraft pulping.

Chapter 2

Aim and Outline of the thesis

2.1 Overarching aim and key research questions

Motivated by the necessity to integrate polymer adsorption with existing pulp mills, this thesis seeks to investigate the fundamentals behind polymer adsorption on cellulose surfaces. A specific focus is placed on the adsorption of carboxymethyl cellulose since it has been demonstrated to significantly enhance tensile characteristics of paper products and aid the production and re-dispersibility of nanocelluloses[12–16]. Besides its implications in different applications, carboxymethyl cellulose adsorption on cellulose is also of scientific significance, as it is a good example of anionic polyelectrolyte adsorption on anionic surfaces. However, the mechanism of adsorption of anionic polyelectrolytes on like-charged surfaces is still ambiguous[9].

This thesis comprises four appended articles, and the first is a review article in which the fundamentals of polymer adsorption on cellulose are discussed, and knowledge gaps are identified (Article 1). The remaining three research articles address the following research questions related to the adsorption of carboxymethyl cellulose on cellulose.

1. What is the driving force for the adsorption of carboxymethyl cellulose on cellulose surface? (Article 3 and a few unpublished results)

2. CMC adsorption is known to be enhanced by the presence of calcium chloride; however, the presence of Ca^{2+} ions are not desired in the pulp mill due to the scaling problems that significantly hamper the smooth operation of the pulp mill. The major challenge in integrating CMC adsorption with current pulp mill is finding an industrially compatible electrolyte system. This challenge drove to the question, how different divalent ions affect the adsorption process? (Article 2 and 3)

3. The role of counterions in the adsorption of CMC is prominent. However, recent investigations suggest that co-ions influence the self-assembly process in cellulose systems; such co-ion effect has not been studied in the case of CMC adsorption or polymer adsorption on cellulose in general. Article 4 in this thesis addresses the question; how does the presence of co-anions influence the adsorption of CMC?

Chapter 3

Background

3.1 Hierarchical structure of wood

Trees are excellent examples of how nature uses molecular, nano, and microscale assembly to form large hierarchical systems. Wood exhibits a variety of structural levels, beginning with the nanoscale construction of the cell wall with biomacromolecules, the subsequent higher level is defined by the organization of the cell wall in terms of cell wall layers with varying structural and chemical compositions. At the microscale, wood tissue is composed of various cell types with varying sizes, shapes, and functions, such as fibers, tracheids (in softwoods), and vessels[17]. At the macroscale, the solid wood body is formed by assembling these tissues. This unique structural organization in wood is obtained via a complex self-assembly process of three major components, namely cellulose, hemicellulose and lignin[18,19]. A schematic diagram of the hierarchical structure of wood is provided in Figure 3.1. Depending upon the wood species, the composition of these cell wall components may vary. In general, cellulose synthase complexes produce and extrude cellulose fibrils with a diameter of roughly 3 nm into the cell wall[20]. These fibrils self-assemble in the matrix of lignin and hemicellulose.

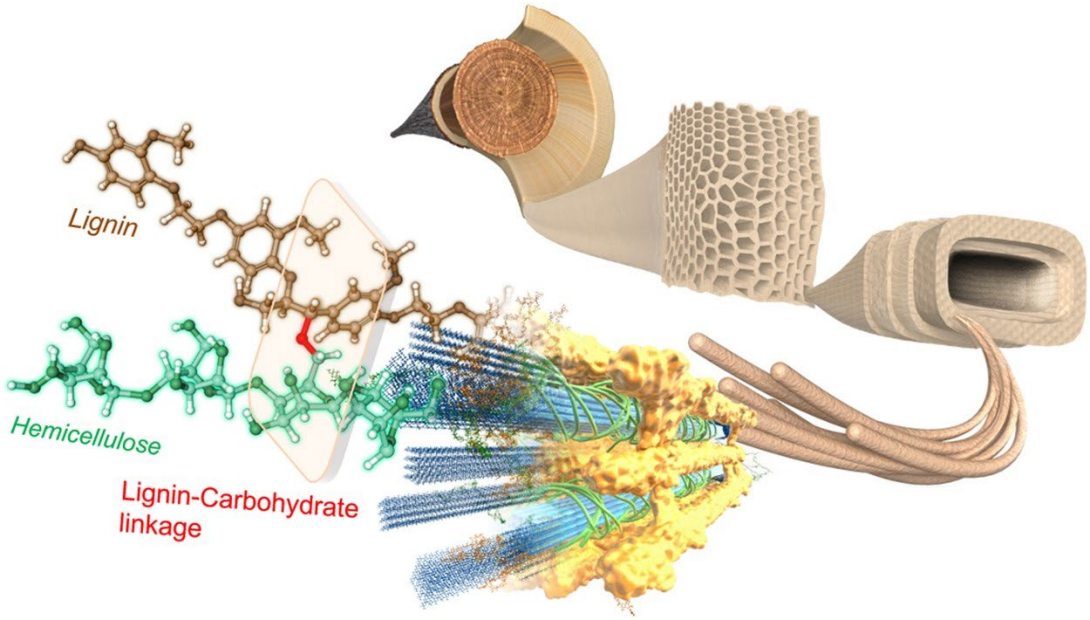

Figure 3.1 Hierarchical structure of wood. by Nishimura et al.[21] is licensed under CC.BY 4.0, reprinted from Springer nature.

3.2 Production of cellulose fibers from wood

Wood fibers have been an important commercial product and a raw material for many paper-based materials. In order to liberate cellulose-rich fibers from the complex wood cell wall structure, various mechanical and chemical treatments have been developed. Mechanical pulping separates fibers from the wood matrix using heat and mechanical treatment, and these fibers retain a large amount of lignin and hemicellulose. Consequently, the yields are relatively high (90%-100%) in mechanical pulping[22]. Chemical pulping separates fibers by dissolving the lignin that glued the fibers together in the cell wall. There are no pulping chemicals that are entirely selective for lignin, and a significant portion of carbohydrates are also affected during the pulping process, resulting in a relatively lower yield when compared to mechanical pulping[22].

Kraft pulping is the widely used chemical pulping technology, and it makes use of a combination of hydroxide and hydrosulphide as active ions to fragment and solubilize lignin[23]. The delignification rate is sensitive to the temperature, an increase of 10 °C of the cooking temperature can speed up the delignification rate two-fold. The cooking temperature can also affect the solubilization of different carbohydrate fractions. A large proportion of glucomannan is dissolved during the initial phase of delignification at temperatures ranging from 100 to 130 °C. Nevertheless, xylans are relatively stable at the initial stage of cooking and start to degrade at slightly greater temperatures, above 140 °C[24]. Considerable decrease in xylan yield at higher temperature is ascribed to degradation due to alkaline hydrolysis and it then promotes so-called secondary peeling reactions[24]. Peeling reactions begin at the reducing end of the carbohydrates. The reducing end may undergo ring-opening; in the presence of alkali, this may result in rearrangements leading to β-elimination, which cleaves off the end group and creates a new reducing end. This peeling will proceed until a stable metasaccharinic acid end group is generated[17]. There is a trade-off between delignification and carbohydrate breakdown in kraft pulping, and conditions are optimized to get an acceptable pulp yield.

While most lignin is dissolved during kraft pulping, a small amount of lignin will remain in the pulp. The residual lignin in kraft pulp significantly differs from the native lignin. In the kraft process, β-O-4' linkages are cleaved, and the residual lignin contains predominantly monolignols connected with carbon-carbon linkages that are stable during kraft cooking and could also be formed via radical coupling reactions. The condensed aromatic rings are believed to be the reason for the intense colour of the kraft pulp.

The pulp used for producing graphic papers and specialized paper products requires high brightness, which can only be obtained by removing the residual lignin using bleaching processes[25]. Because the bleaching efficiency of a single bleaching stage decreases with time, bleaching treatments are typically carried out in stages.[25,26] This improves selectivity and yield while minimizing degradation reactions of carbohydrates. The pulp obtained by sequential bleaching is brighter than the one that obtained with a single stage. The first bleaching procedure for pulp was established in 1774, and it used chlorine (Cl2) as an active bleaching chemical. Then hypochlorite (OCl^-) based bleaching process was developed, but these were gradually discontinued in favour of more environmentally friendly bleaching chemicals such as chlorine dioxide (ClO_2), hydrogen peroxide (H_2O_2), oxygen (O_2), and ozone (O_3). Modern bleaching sequences are often classified as either elemental chlorine-free (ECF), which means that no elemental chlorine gas is used during the bleaching, or Totally chlorine-free (TCF).

3.3 Ultrastructure of cellulose fibers

Typically, in plant cells the cellulose is arranged in different layers with different orientations and densities[18]. The schematic of the layered structure of fiber wall is presented in Figure 3.2.

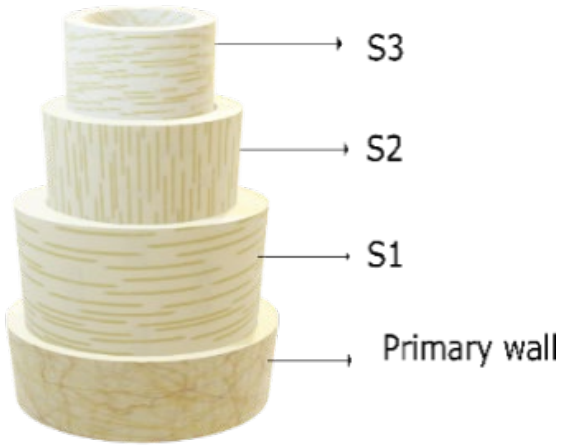

Figure 3.2 The schematic of the layered structure of fiber wall; S1, S2, and S3 are secondary cell wall layers.

The native state of cellulose has a very low void volume (0.02 cm^3/g) due to the compact arrangement of cellulose within the lignin hemicellulose matrix[27]. When cell wall components are removed, the void volume increases as a result of formation of pores of varying sizers ranging from nano meters to micro meter dimensions[27–29]. The change in void volume is substantial when the remaining

traces of lignin in the fiber wall are removed by bleaching. The bleached fibers will have an open, porous structure, which will enhance the fiber's surface area[30]. These structural changes have significant effect on the ability of the fibers to adhere to one another during drying of the paper, and hence on the strength of papers made from the fibers[31]. Furthermore, the change in pore size of the fiber wall influence the diffusion of molecules across the fiber wall. This is particularly important when discussing chemical modifications and polymer adsorption on cellulose fibers[8,32].

3.4 Chemical modification of cellulose fibers

Cellulose fibers possess physical robustness and chemical stability, stemming from their unique supramolecular structure. However, the need for new material applications based on cellulose requires increased functional diversity, and various functionalization approaches have been developed, using both chemical and physical procedures[8,33,34]. Chemical modification of cellulose usually involves converting hydroxyl groups in the cellulose chains into ethers, esters and acids. Figure 3.3. depicts the chemical modification routes of cellulose.

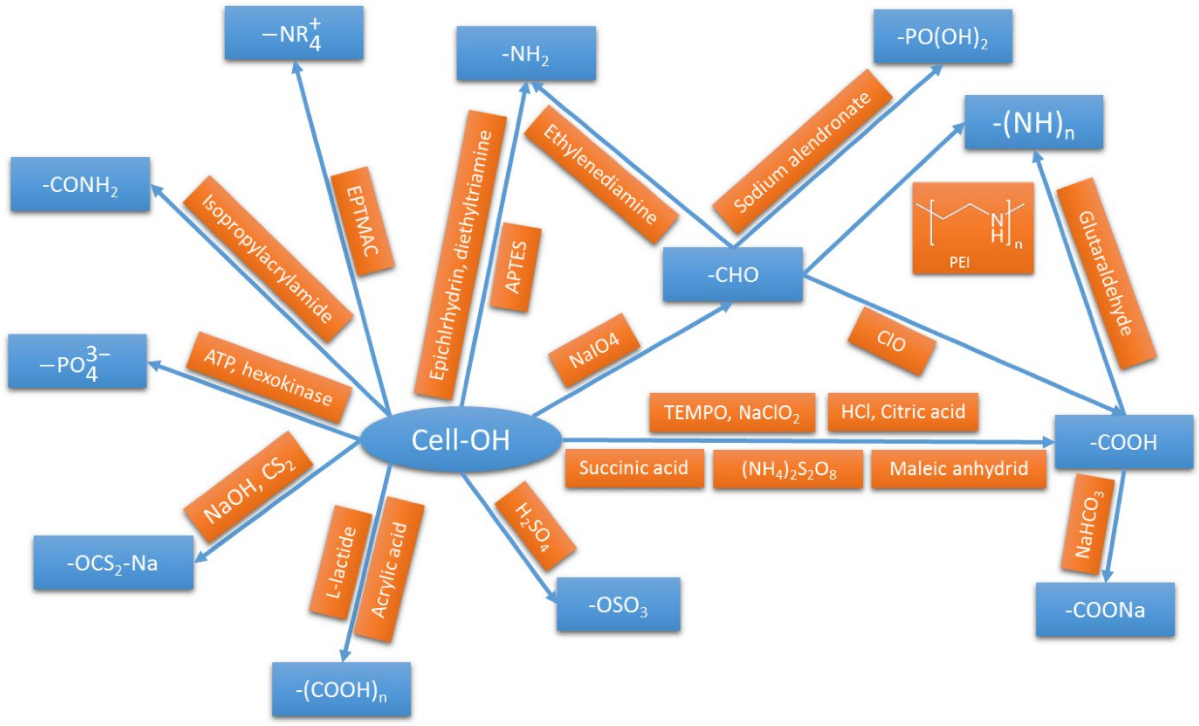

Figure 3.3 Chemical modification routes for cellulose by Voisin et al.[35] licenced under CC.BY 2.0, reprinted from MDPI.

The inherent reactivity of hydroxyl groups is less important in chemical reactions of cellulose since the accessibility of reagents is predominantly regulated by the supramolecular structure when the reactions are performed on fiber[8]. Cellulose reactions can be carried out in cellulose solutions in which the

supramolecular structure has completely disappeared[36–38]. However, the majority of industrial chemical reactions are heterogeneous or are, at least, to begin with, and the supramolecular structure is changed as the reaction progresses. Non-uniform substitutions are typically produced by heterogeneous reactions, with a predilection for accessible low-ordered areas. To some extent, swelling media can improve accessibility and ensure substituents' uniform distribution. However, in non-swelling media, the reactions are mainly limited to the surface, which is desired for applications where the fiber morphology needs to be retained. The location of functional groups in cellulose fibers is critical in allowing fiber-fiber bonding and the formation of a strong fiber network[12]. Papers manufactured with toposelectively carboxylated cellulose fibers in non-swelling environments, such as an isopropanol-methanol mixture, exhibited improved tensile strength compared to unmodified fibers[39,40]. However, due to environmental considerations, the use of non-swelling media for topochemical reactions is restricted in practice.

3.5 Non-covalent modification of cellulose fibers

Polymer adsorption can modify the surface of the fibers without compromising their physical integrity. Furthermore, unlike covalent cellulose modification, the non-covalent modification technique can be restricted predominantly to the surface by using polymers with large molecular weights[41]. Adsorption of polymers has been used in the paper industry for a long time as retention aids and strength additives. For example, xylan recirculation has been utilized to boost pulp yield for many years, and the critical phenomenon involved in this process is xylan adsorption on the fiber surface[42,43]. Recently, it has been shown that the polymer adsorption step can be integrated into the kraft pulping process to enable resource-efficient modification of cellulose fibers[11,13].

3.5.1 Model cellulose surfaces for adsorption studies

Interest in polymer adsorption on cellulose has grown in recent years as new areas of application, such as healthcare materials and diagnostic platforms, have demonstrated a greater need for functionalized bio-based surfaces with controlled surface properties[44,45]. Understanding the polymer adsorption process and the features of the adsorbed layer is thus required for designing the next generation of cellulose-based products, and fundamental polymer adsorption investigations are still necessary.

Cellulose materials derived from pulping operations typically contain residual levels of other wood components and negative charges derived from the pulping process[46]. Thus, cellulose fibers always contain negative charges, although they are frequently considered uncharged if not further functionalized. Furthermore,

the distribution of these charges in cellulose fibers is heterogeneous. Because of cellulose fibres' chemical and structural heterogeneity, it is challenging to extract the underlying mechanism of polymer adsorption on cellulose fibers[10].

Cohen Stuart et al.[47] stated that an optimal surface for fundamental adsorption experiments should meet the following criteria:

- The chemical composition of the surface should be fully understood.
- The substrate's surface charges should be thoroughly characterized.
- The surface's morphological structure, including surface roughness and porosity, should be well-characterized.
- The surface's curvature should be determined.
- The exposed surface's crystallinity should be known.
- There should be no material exchange across the solid/liquid contact.

Even though cellulose surfaces are not ideal for fundamental adsorption studies, there has been a need to understand the physicochemical interactions between polymers with cellulose surfaces. This necessitates the use of precise surface sensitive techniques such as Quartz Crystal Microbalance with Dissipation (QCM-D), Surface Plasmon Resonance Spectroscopy (SPR), ellipsometry and neutron reflectivity. QCM-D is one of the primary analytical techniques utilized in this thesis, and a detailed discussion on this technique and methods are included later in this chapter.

Surface sensitive analytics, with detection limits in ng cm^{-2}, require substrates that conform to the Cohen Stuart et al. standards[47]. Cellulose model surfaces have been designed to overcome the limitations associated with the use of cellulose macrofibers as a substrate in fundamental research. Langmuir-Blodgett (LB) deposition and spin coating have been the primary methods for creating cellulose model films[48,49]. The requirement that the depositing materials be liquid is a limitation for both methods. Given cellulose's insolubility in most common solvents, producing cellulose model surfaces using these techniques is difficult. Trifluoroaceticacid (TFA), N-methylmorpholine N-oxide (NNMO), and urea-sodium hydroxide (NaOH) mixes have all been used to dissolve cellulose and deposit it on silica and mica substrates[50,51]. However, these films do not represent the native form of cellulose (cellulose I) in terms of crystallinity or crystalline structure, but rather cellulose II. An additional strategy for producing cellulose model film surfaces is to spin-coat cellulose derivatives followed by regeneration to cellulose by cleaving away the substituents on the surfaces: in this case, selectivity, efficiency, and ease of regeneration are all critical. Trimethylsilyl cellulose (TMSC) films are often used to prepare regenerated model films[52–55]. The spin coated TMSC films are exposed to HCl vapour to form regenerated cellulose[56]. The chemical reaction scheme is depicted in Figure 3.4.

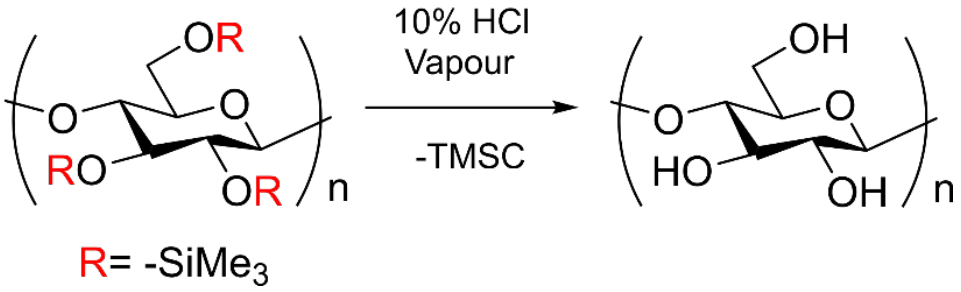

Figure 3.4 Regeneration reaction of cellulose from trimethylsilylcellulose in the presence of HCl vapour.

The regenerated cellulose model films exhibit diffraction characteristics and exhibit some crystalline organization, but not to the same as cellulose I[52,57]. Another possibility is to spin-coat colloidal suspensions of nanocellulose, either cellulose nanocrystals (CNC) or cellulose nanofibers (CNF), onto a silica substrate to create ultrathin cellulose model films that are more akin to and representative of native cellulose[58](see Figure 3.5). A very thin anchoring layer made of polyethyleneimine (PEI) or aminopropyltriethylsilane (APTES) is often used to improve the adhesion of cellulose nanofibrils to the silica substrate[59,60].

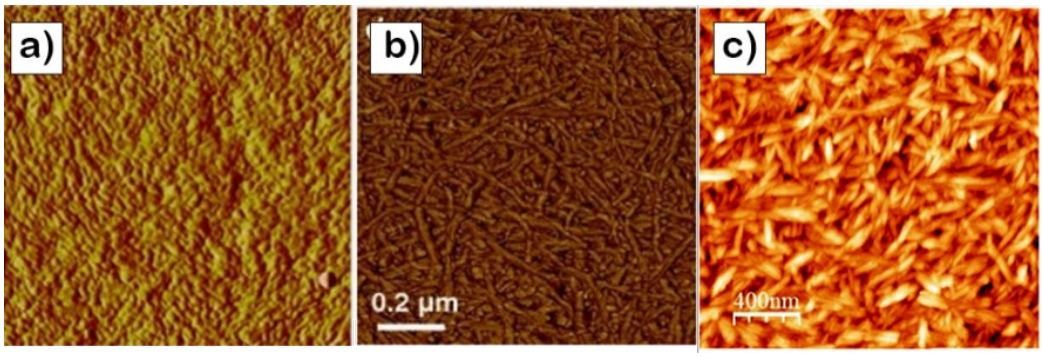

Figure 3.5 AFM micrograph of different cellulose model films prepared by spin coating. a) Regenerated cellulose films from TMSC reprinted from Niegelhell et al.[61] with permission from Elsevier, b) CNF model films with an anchoring layer of polyethyleneimine reprinted from Nypelö et al.[60] with permission from Springer and c) CNC model films reprinted from Villares et al.[62] with permission from Royal Society of Chemistry.

In this thesis, the cellulose model films were prepared by spin coating CNF suspension on a silica coated QCM-D sensor. PEI is used as an anchoring layer. The specifications of CNF used in this thesis is given in Appendix (section 1) and detailed description of film preparation and characterization is also provided in Appendix (section 2).

3.5.2 Polyelectrolyte adsorption theory

Collective efforts of Scheutjen, Fleer and Stuart resulted in a lattice model based self-consistent field theory to explain the polymer adsorption process. In this theoretical treatment, adsorption of polymer is described in terms of four different parameters: χ, χ_s, q_m, σ_0, where χ and χ_s are the Flory-Huggins parameters accounting for the polymer-solvent interactions and the polymer segment-surface interaction, respectively. Both χ and χ_s have a positive linear dependence on the amount adsorbed. The terms q_m and σ_0 represent the surface charge and polymer segmental charge, respectively, and account for the Coulombic interactions in polyelectrolyte adsorption (q_m.and σ_0 are only used for polyelectrolyte adsorptions). The Scheutjens and Fleer theory can effectively predict the adsorption behaviour of different polymers, polymer adsorption isotherms, segmental density distributions and "tail-and-train" distributions. In the following section, different cases of polyelectrolyte adsorption on cellulose will be discussed from a theoretical perspective.

3.5.3 Polyelectrolyte adsorption on cellulose

3.5.3a Adsorption of cationic polyelectrolytes on cellulose

Adsorption of positively charged polymers on cellulose is critical in paper manufacturing since they are employed as additives to enhance the performance of the paper and as a retention aid. Consequently, numerous experiments have been conducted to investigate the adsorption behaviour of cationic polyelectrolytes on cellulose fibers. A review by Wågberg connected the various scenarios anticipated by Scheutjens and Fleers' theory to available data on the adsorption of primarily positively charged polyelectrolytes on cellulose fibers at the time[32].

The porous nature of the cellulose fibers makes the explanation of adsorption processes difficult[10]. Given the presence of charged groups on the surface and in the cell wall of fibers, it was believed that electrostatic interactions govern polyelectrolyte adsorption. It has been demonstrated that the adsorption of highly charged cationic polyelectrolytes occurs at a 1:1 charge stoichiometry in the absence of an electrolyte, this type of adsorption is generally known as electro-sorption where the segmental charge density (σ_0) and surface charge (q_m) are most important[63]. With an increase in electrolyte concentration, the adsorption decreases, the decrease in adsorption of polyelectrolytes is ascribed to the screening of segmental charge of the polyelectrolyte and surface charge of the fiber. However, in moderate electrolyte concentration, adsorption may start to increase; this could be attributed to the adsorption of polyelectrolytes in coiled

conformation. Further increase in electrolyte concentration decreases the adsorption[64].

Recently, it has been demonstrated that the oppositely charged polyelectrolyte association in water is driven by entropic factors such as the release of counterions and water[65]. Thus, the adsorption of cationic polyelectrolytes on the surface of cellulose cannot be attributed to electrostatic interaction; rather, the predominant driving factor is the release of counterions. (see Figure 3.6). The increase in salt concentration in the system reduces the entropy gain resulting in a decrease in the adsorption[66].

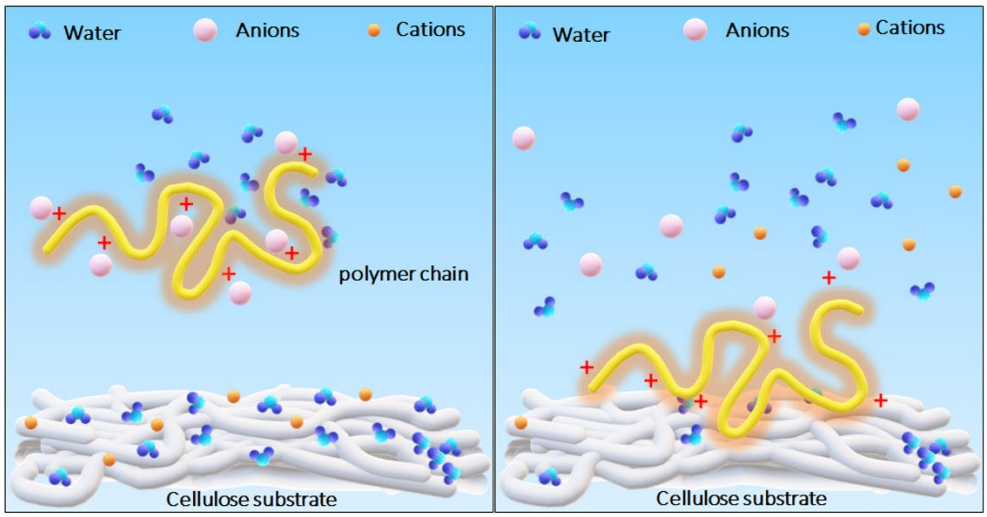

Figure 3.6 Diagram illustrating the adsorption of cationic polymers on a cellulose surface, driven by the release of counterions. by Arumughan et al.[9] licenced under CC BY 4.0, reprinted from Elsevier.

3.5.3b Adsorption of anionic polyelectrolytes on cellulose

As previously stated, the surface of cellulose is negatively charged due to the presence of residual amount of other wood components such as hemicelluloses, extractives, and oxidized groups created during the pulping process. Electrostatic repulsion should dominate the interactions of anionic polyelectrolytes with the cellulose surface, unless these electrostatic forces are overcome by other chemical interactions. The electrostatic repulsion between the surface and polyelectrolyte can be reduced by adding salts into the system, thus tuning the adsorption process. For the specific case of anionic polyelectrolyte adsorption on a like-charged surface, a simulated adsorption isotherm according to Scheutjens-Fleer theory (S-F theory) is depicted in Figure 3.7. It is important to keep in mind that this model only considers the addition of monovalent salts with an ionic strength equal to the salt concentration.

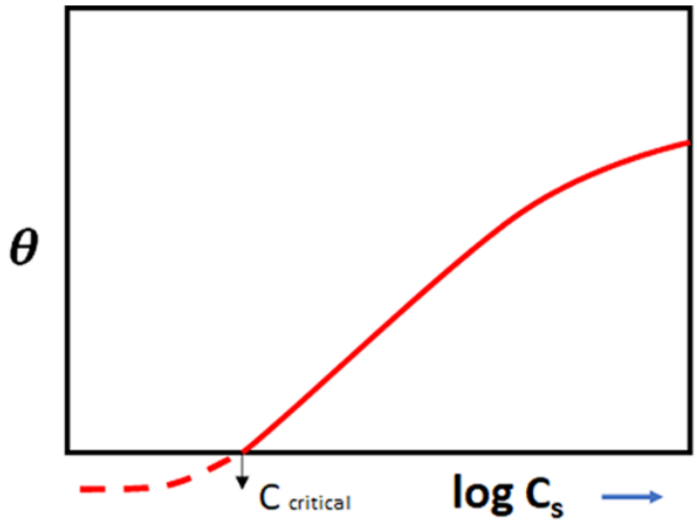

Figure 3.7 A predicted adsorption isotherm of a negatively charged polymer on a like-charged surface. θ : amount adsorbed and C_s: concentration of monovalent salt Adapted from Fleer et al.[67]. by Arumughan et al.[9], licenced under CC BY 4.0, reprinted from Elsevier.

The dotted line in the figure demonstrates that at lower salt concentrations, the electrostatic repulsion dominates, and no adsorption occurs: this is commonly referred to as depletion. The charges on the polymer and the surface are screened by the cations in the salt solution at a critical salt concentration, $C_{critical}$, and depletion is converted to adsorption. At increasing salt concentrations, the repulsive electrostatic forces' contribution to adsorption energy diminishes, and non-electrostatic forces dominate adsorption. This is referred to as "screening enhanced adsorptions" by van de Steeg[68].

3.5.4 Tools to study the polymer adsorption

There are various tools available to investigate adsorption depending on the substrate type and type of the adsorbing polymer. Therefore, the discussion under this heading is divided into two sections, the first discusses polymer adsorption on cellulose macrofibers, and the second discusses polymer adsorption on cellulose model films.

3.5.4a Adsorption of polymers on cellulose macrofibers

There are various methodologies available to study the adsorption of polymers on cellulose pulp fibers. The technique used for adsorption investigations is determined by the type of adsorbing polymers investigated. For adsorption of polyelectrolytes, titration techniques are predominantly used[32,63,64,69,70]. These titration techniques include both direct and indirect titrations. Direct

polyelectrolyte titrations measure the charges introduced by adsorbed polyelectrolytes in order to calculate their amount; this is performed by titrating the modified fibers with an oppositely charged polyelectrolyte titrant whose structure and molecular weight are known. By assuming a stochiometric neutralization, polyelectrolytes adsorbed on fibers can be determined volumetrically as long as a method for detecting the equivalence point is available.

Conductometric titrations with NaOH can quantify the amount of adsorbed polyelectrolytes if they include acidic groups[41]. Titrations with polyelectrolytes and conductometric titrations with NaOH as the titrant are frequently used in conjunction to analyse adsorption since these techniques probe the charges in the fibers at distinct structural levels[41,71]. Titrations using polyelectrolytes with a high molecular weight measure charges localized on the surface (surface charge analysis), while conductometric titrations utilizing NaOH measure charges distributed both inside and outside the fiber wall due to the hydroxide ions' increased accessibility (termed as total charge analysis). In article 2 surface charge measurements and total charge measurements were combined to better understand the distribution of adsorbed CMCs on fibers. For experimental details, readers are referred to appended article 2 or Appendix (section 3 to 6).

Alternatively, adsorption of polymers on cellulose surface can be qualitatively and quantitatively assessed indirectly by looking at how much CMC is left in the solution after the adsorption via methods such as Total Organic Carbon (TOC) measurements, polyelectrolyte titrations. These techniques have been used in Article 2, the experimental details and results are provided in Appendix (section 7).

3.5.4b Adsorption of polymers on cellulose model surfaces

The development of cellulose model surfaces enables the application of surface-sensitive techniques such as ellipsometry, SPR, Stagnation Point Adsorption Reflectometry (SPAR), and QCM-D for real-time probing of polymer adsorption on cellulose surfaces. Ellipsometry, SPR, and SPAR are based on optical response and can be used to precisely determine the amount of dry mass adsorbed on a surface, whereas QCM-D is an acoustic approach that determines the aerial mass of the adsorbed polymer layer and any associated solvent. In this thesis, QCM-D was utilized extensively to characterize prepared model surfaces and investigate the adsorption of CMC. Furthermore, viscoelastic nature of the adsorbed layers was also probed using QCM-D. A detailed description of methods is given in Appendix (section 2 and 8).

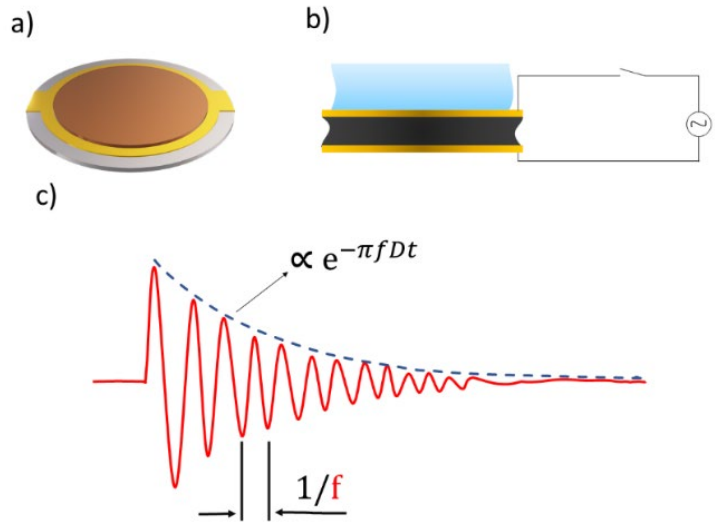

Figure 3.8 a) An illustration representing a QCM-D sensor. b) Illustration of vibration of the crystal when an electric field is applied. c) Decay of stored energy with respect to time.

The main component of QCM-D is a quartz crystal sensor coated with either gold or silica (see Figure 3.8a). Quartz crystals are piezoelectric, an oscillating electric field is applied across the material induces vibrations at its resonance frequency (see Figure 3.8b). The frequency of vibration of the crystal is directly proportional to the mass associated with the crystal surface. Therefore, the frequency change during the adsorption events can be translated into adsorbed mass using the Saurebrey relation:

$$\Delta m = -(C_{QCM}/n)\,\Delta f \qquad (1)$$

where Δm is the areal mass change, C_{QCM} is the mass sensitivity constant (C_{QCM}= 17.7 ng cm^2 Hz^{-1} at f = 5 MHz), n is the overtone number, and Δf is the frequency change. However, the Sauerbrey relation only holds when adsorbed layers are rigid.

The adsorbed layers are usually not rigid when hydrophilic polymers and biomacromolecules are adsorbed. Instead, these layers will have a significant viscous component that attenuates the resonance frequency response of the crystal due to fast energy dissipation (see Figure 3.8c). QCM instrument monitor this energy dissipation to provide useful information about the viscoelastic properties of the adsorbed layer. The dissipation factor D_n is defined as:

$$D_n = \frac{1}{\pi f_n \tau} \qquad (2)$$

where τ is the rate at which the amplitude decays when the driving AC-voltage is shut off.

In the case of adsorption of polyelectrolytes on cellulose surfaces, the adsorbed layers are often viscoelastic[52,53], and the viscoelastic nature of the adsorbed layer should be considered while calculating the adsorbed mass. Johannsmann's model accounts for the viscoelastic nature of the film while calculating the adsorbed mass. According to Johannsmann, the shift in the complex frequency is related to the resonance frequency of the crystal in solution by the following equation.

$$\hat{\delta}f \approx -f_0 \frac{1}{\pi\sqrt{\rho_q \mu_q}} \left(f\rho d + \hat{\jmath}(f) \frac{f^3 \rho^2 d^3}{3} \right) \tag{3}$$

where $\hat{\delta}f$ is the shift in the complex frequency, f_0 is the fundamental resonance frequency of the quartz crystal in air, f is the resonance frequency of the crystal in contact with the solution, d is the thickness of the film and $\hat{\jmath}(f)$ is the complex shear compliance. ρ_q and μ_q are the specific density and elastic shear modulus of the quartz crystal, respectively. Equation (3) can be written in a simpler form by using equivalent mass (m*) which is defined as:

$$m^* = -\frac{\sqrt{\rho_q \mu_q}}{2f_o} \frac{\hat{\delta}f}{f} \tag{4}$$

and then we obtain a linear equation

$$m^* = m^o \left(1 + \hat{\jmath}(f) \frac{f^2 d^2 \rho}{3} \right) \tag{5}$$

It is assumed that $\hat{\jmath}(f)$ is independent of frequency in the accessible range and the true sensed mass m^o is obtained graphically by plotting equivalent mass against the square of the resonance frequency. It is important to mention that the true sensed mass calculated using Johannsmann's modelling includes the mass of water that is associated with the adsorbed layer and thus not equal to the dry mass of the adsorbed polymer.

3.5.5 Adsorption of carboxymethyl cellulose on cellulose

Carboxymethyl cellulose (CMC) is a negatively charged water-soluble polyelectrolyte produced by carboxymethylation of cellulose[72,73]. The chemical structure of CMC is provided in Figure 3.9. It has a wide range of applications in pharmaceutical products, foods, mineral processing, paper making etc. In these applications, the solubility of CMC in water is critical. It is well established that the degree of substitution (DS) and the molecular size of the CMC have a

significant effect on its solubility[74]. In CMC, three hydroxyl groups (placed at the C2-, C3-, and C6 positions) of each anhydroglucose unit are theoretically available for carboxymethyl group substitutions. Thus, the highest possible value of DS (average number of substituent groups per monomer unit) is 3.0. Generally, CMC must have a DS value greater than 0.6 to be water-soluble. Adsorption of CMC on solid surfaces is vital in some applications, especially in mineral processing and paper making[12,75–77].

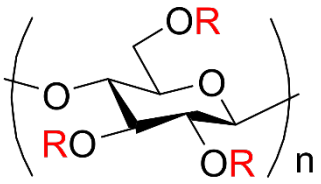

$R = H \text{ or } -CH_2COO^-Na^+$

Figure 3.9 Chemical structure of sodium carboxymethyl cellulose.

CMC adsorption on the surface of cellulose has been investigated because it is a resource-efficient method to increase the number of carboxylic groups on the fiber surface. The presence of charges on fibers substantially impacts unit operations in paper making and the final qualities of the papers produced. The adsorption of high molecular weight CMC has been shown to introduce charges toposelectively on the fibers, resulting in significant increases in tensile characteristics of the paper. A seminal work of CMC adsorption on cellulose fiber was carried out by Laine et al.[12,41], who found that increasing the electrolyte concentration in the system increased the attachment of CMC onto the fiber surface, as shown in Figure 3.9.

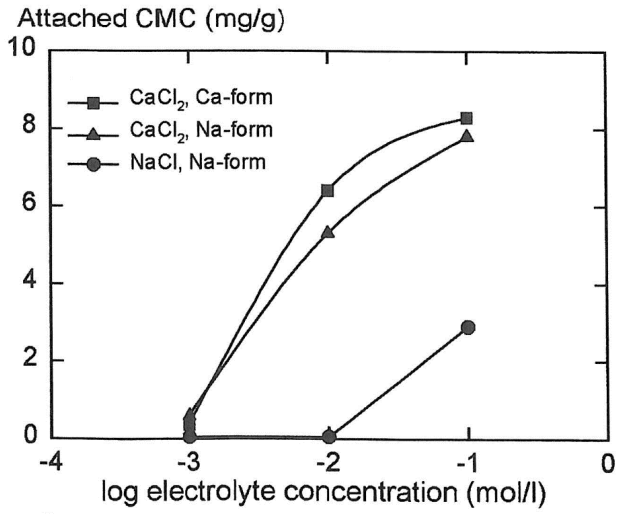

Figure 3.10 Adsorption of CMC on cellulose fibers (Ion exchanged with Ca^{2+} and Na^+) as a function of electrolyte concentration. Reprinted from Laine et al.[41] with permission from De Gruyter.

This binding isotherm has a shape comparable to that predicted by Fleer et al. (Figure 3.7), and no adsorption can be detected at low salt concentrations (i.e., no added electrolyte). This corresponds to depletion phenomenon predicted by Fleer et al.[67]. Figure 3.10 demonstrates that the valency of the cations in the electrolyte has a significant impact on the adsorption process. The critical salt concentration needed to facilitate adsorption is relatively small for $CaCl_2$ compared to NaCl, this clearly shows that divalent ions such as Ca^{2+} ions have an extra contribution to the adsorption.

Temperature, pH and the degree of substitution (DS) of the CMC have all been demonstrated to influence the adsorption process. Adsorption was observed to be improved at low pH (near to pH 2)[52]. The improved adsorption was ascribed to full protonation of carboxylic groups in the CMC and decreased polyelectrolyte solubility[52]. The pH of the solution influences the CMC chains and the cellulose surface: a lower pH reduces the segmental charge of the CMC chains and the surface charge of the cellulose fiber (q_m). The lower DS of CMC promoted the adsorption due to the lower segmental charge and reduced solubility. Laine et al.[41] also discovered that: higher temperatures favoured the CMC adsorption and resulted in higher quantities being attached.

Because of the structural similarity of the backbones of CMC and cellulose, a co-crystallization mechanism for the irreversible attachment of CMCs on cellulose surfaces has been proposed in the literature[41]. However, the interactions that govern this co-crystallization process are unknown. Kargl et al. [52]. investigated the adsorption of CMC on cellulose model surfaces with variable chemical compositions, including regenerated cellulose from TMSC, deacetylated cellulose acetate, and cellulose acetate, at various pH levels. They discovered a pH-dependent adsorption trend in both deacetylated and regenerated TMSC cellulose films, which they attributed to the involvement of specific interactions between CMCs and the cellulose surface. This is consistent with Scheutjens and Fleers' assumption that the adsorption of polyelectrolytes on like-charged surfaces is governed by non-electrostatic forces, as seen in Figure 3.11.

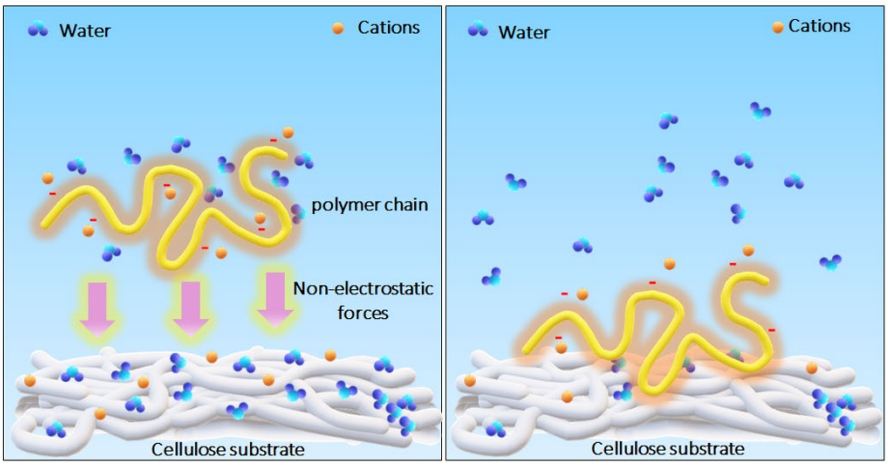

Figure 3.11 Illustration of the involvement of non-electrostatic forces in polyelectrolyte adsorption on a like-charged surface. by Arumughan et al.[9], licenced under CC BY 4.0, reprinted from Elsevier.

In another adsorption study using regenerated model cellulose surfaces by Liu et al.[53], adsorption was monitored using QCM-D and SPR. Combining these two techniques provided quantification of the adsorption based on both gravimetric and optical responses. In this study, it was observed that, when compared to NaCl, $CaCl_2$ enhanced the adsorption of CMC at the same ionic strength.

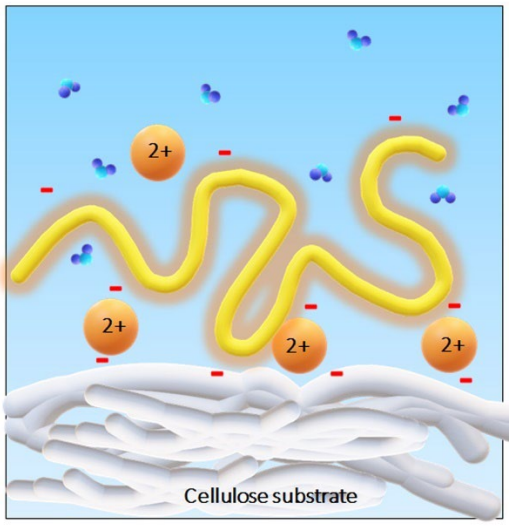

Figure 3.12 Diagram illustrating bridging between an anionic polyelectrolyte and cellulose fibers, mediated by calcium ions. by Arumughan et al.[9], licenced under CC BY 4.0, reprinted from Elsevier.

The authors suggested that the presence of Ca^{2+} ions in the solution provided a strong bridge between the CMC chains and regenerated cellulose surface, as depicted in Figure 3.12. Theoretical investigations suggest that multivalent ions such as calcium ions can overcharge the surface or polymer chains to cause a charge inversion and thereby facilitate anionic polyelectrolyte adsorption on

anionic surface[78]. Tirafferi et al. experimentally supported this claim in the case of adsorption of polystyrene sulfonate on silica [79]. However, such multivalent ion-induced charge inversion has not been reported so far in the case of cellulose systems.

3.6 Charged interfaces in aqueous electrolyte solutions

In the previous section, we briefly discussed the fundamental aspects of polymer adsorption and reviewed the literature on the adsorption of CMC on cellulose surfaces. We have seen that the addition of salts can modulate the adsorption behaviour of CMC. Mainly, it was found that the adsorption behaviour changes with the valency of counterions. This section will discuss how ions behave at a charged interface in an aqueous solution. When a charged surface is introduced into an aqueous electrolyte solution, oppositely charged ions from the bulk are drawn towards the interface due to electrostatic attraction. As a result, a spatially inhomogeneous charge distribution along the surface normal emerges. The electric field generated by the charges on the surface can interact with static dipoles in water molecules, causing them to preferentially orient in the vicinity of the interface. Due to this reason, the water molecules at the interface will behave differently than the water molecules in bulk, and the water no longer acts as a continuum (the interfacial water has a reduced dielectric constant)[80]. Together with the water molecules and the interfacial ion distribution forms the electrical double layer (EDL).

Helmholtz was the first to offer a model for the EDL in 1853[82], describing it as a parallel-plate capacitor with one plate representing the highly charged interface and the other representing the centre of the closest approaching hydrated counterions (the outer Helmholtz plane, OHP)[82,83]. These two plates create the Helmholtz layer (also referred to as the Stern layer), a region in which the potential falls linearly. Helmholtz's model did not account for the specifically adsorbed partially solvated ions; Grahame refined the Helmholtz model by considering these adsorbed ions and introducing an inner Helmholtz plane (IHP) concept to the model[84]. Later, Gouy and Chapman introduced a model using the Poisson-Boltzmann equation to describe the distribution of ions from the interface. The major assumptions in this mean-field description of the interface were that the surface is considered smooth and has a uniform charge distribution, the ions are simply point charges and all interactions are governed by electrostatics and there are no ion-ion correlations. Additionally, this model assumes water as a dielectric continuum[85,86]. Gouy-Chapman model could explain many experimental observations. However, one of the major shortcomings of this model was the assumption that ions are point charges that can approach the interface at an infinitesimally small distance in high fields.

This assumption was unrealistic due to the fact that ions have a finite size, hydration shells and also solvation effects[87]. By merging the Helmholtz and Gouy–Chapman models, the Stern model incorporates finite-sized ions and accounts for a lower interfacial water dielectric constant[88]. The Gouy–Chapman diffuse layer is located beyond the OHP in this model. The Stern model is frequently referred to as the Gouy–Chapman–Stern (GCS) model, as illustrated in Fig. 3.13.

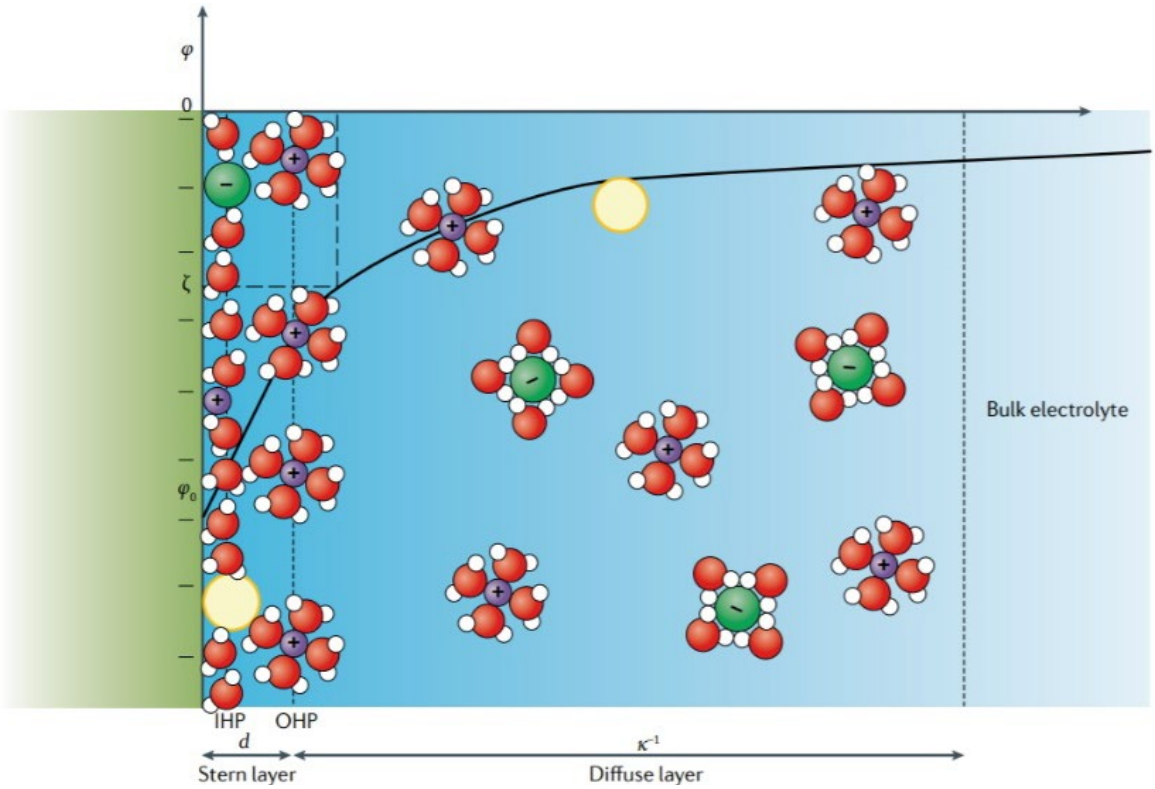

Figure 3.13 Schematic description of the Gouy–Chapman–Stern model. Indicated are the inner Helmholtz plane (IHP), the outer Helmholtz plane (OHP), the thickness of the Stern layer, d, and the thickness of the diffuse layer, also known as the Debye length, κ^{-1}. Also indicated is the potential φ as a function of the distance from the surface. The purple, green, and yellow spheres represent the cations, anions, and neutral species. Hydration water is explicitly depicted both around the ions and at the surface. Reprinted from Gonella et al.[81] with permission from Springer Nature.

3.7 Specific ion effects

In the previous section, I briefly discussed various models that describe a charged solid-liquid interface in an aqueous media. The spatial distribution of ions at a charged interface is critical in determining how charge affects water organization. The differences in water organisation have consequences in many biological and non-biological interfacial processes such as energy storage[89–92].

We have seen in the previous section that in mean-field models, the water is considered an electrostatic continuum. This can be true if we assume an ideal electrolyte solution that behaves like an infinitely dilute system. However, at high concentrations of salts (~0.1 M), water cannot be considered a continuum. Rather than that, water molecules in the hydration shells are shared, and the solvent takes on the characteristics of a linked matrix[93]. At concentrations greater than 1M this effect will become more prominent and no "free water molecules" remain available due to the dense packing of the hydrated ions. As a result, ion-ion, ion-solvent, and solvent-solvent interactions cannot be ignored. This introduces ion specific interactions where physicochemical properties of the systems are dictated by the identity of the ions present in the system[94–97].

The first systematic study on ion-specific effects dated to 1888 by Francis Hofmeister[98,99]. He studied the precipitation of egg yolk protein in the presence of salts. For salts containing the same cation, he ranked the anions according to their ability to precipitate the protein, while fixing the anion yielded a ranking for the cations, which together form the framework of the Hofmeister series (see Figure 3.14).

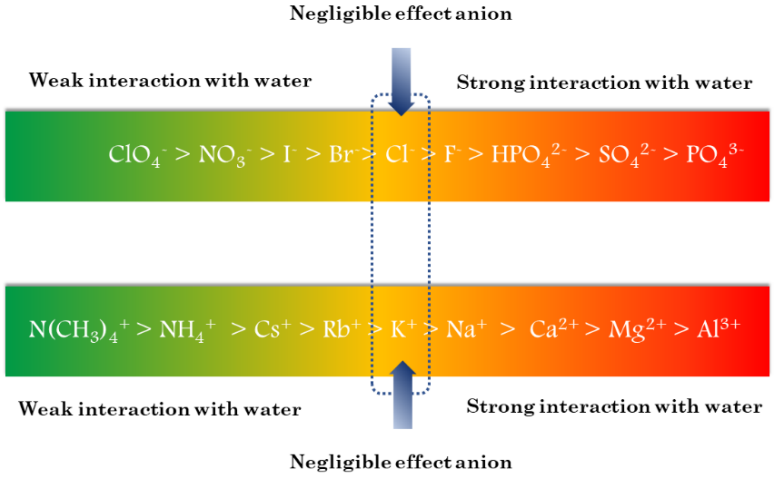

Figure 3.14 Hofmeister series of anions and cations.

Ion specificity is reflected in several easily quantifiable physicochemical properties of aqueous salt solutions for example, the viscosity of the salt solution.

Jones and Dole studied the viscosity of aqueous solutions of different salts[100]. They discovered that depending on the nature of the salts, salt solutions could be either more or less viscous than pure water. The relative viscosity (η/η_0) is related to the salt concentration c by the following equation:

$$\eta/\eta_0 = 1 + A\sqrt{c} + Bc \qquad (6)$$

where A is the electrostatic parameter, and B is the ion-specific parameter, also referred to as Jones-Dole viscosity coefficient. Determining the Jones-Dole coefficient for salt is an excellent way to quantify the specific interaction of ions with water. Ions with a positive B value are termed kosmotropic ions (structure makers), the presence of these ions in water results in higher viscosity than water. In contrast, ions that result in saline solutions with viscosity less than water are called chaotropic ions, which have a negative value of the Jones-Dole coefficient.

Based on the aforementioned classification of ions into kosmotropes and chaotropes, one possible explanation for Hofmeister's observation (salt-induced protein precipitation) is that kosmotropic anions withdraw water molecules out of the hydration layer of proteins, forcing them to precipitate; chaotropic anions are thought to use the opposite mechanism[98,99]. Although this appeared to be a qualitatively satisfactory explanation, many observations reveal that the exact mechanism in operation is much more complex. The following paragraphs outline some of these observations.

The 'water withdrawing mechanism' could successfully explain the anion behaviour in protein precipitation observed by Hofmeister. However, when it comes to cations, salts with kosmotropic cations have been shown to be 'salting in' proteins and chaotropic cations' salting out' the protein[101]. This observation is exactly opposite to the effect of Hofmeister anions[102]. Another reason for questioning the 'water withdrawing' mechanism is that the Hofmeister series was observed to reverse the order in some cases. The normal Hofmeister series is usually valid for proteins when the pH value is above the isoelectric point (IEP) of the proteins. However, the trend reverses when the pH is just below the IEP (this trend is referred to as reverse or inverse Hofmeister series)[96,103]. A pH below IEP makes the series go from 'inverse' to 'direct' with more salt[104]. Several investigations have established that ions have almost no effect on water's hydrogen bonding beyond their first solvation shell[105]. As a result, the hypothesised long-range effect of ions on the structure of water has been abandoned. Similarly, the old mechanism ascribed Hofmeister effects to salt-

induced water removal from protein surfaces is no longer an adequate explanation for ion-specific occurrences at salt concentrations below 0.2 M[96].

The extensive works in colloids and interface science, primarily related to lipid bilayers and surfactant systems, gave more insights into specific ion effects. However, specific ion-ion and ion-surface interactions must first be disentangled to understand the examined ion-specific phenomenon (electrolyte activities, colloid phase transition, protein aggregation, enzyme activities, etc.)[102]. To put it another way, we need to know which laws, or at least empirical rules, are applicable to the system of interest. The two primary approaches are the Law of Matchmaking Water Affinities (LMWA) and dispersion forces.

3.7.1 Law of Matchmaking Water Affinities (LMWA)

Collins devised an empirical rule that established a previously missing systematic framework for ion-ion and ion-charged site interactions[106]. LMWA begins with the traditional classification of ions as kosmotropes and chaotropes. However, the terms kosmotrope and chaotrope are no longer used to describe how ions could alter the bulk water structure; they are now used to describe ions 'degree of hydration'. Generally, kosmotropes are highly hydrated ions, and chaotropes are less hydrated. Then, it has been recognised that ions of opposite charge tend to form ion pairs[107]. According to Collin's LMWA, the ion pair is stable when the cation and anions that undergo ion-pairing have similar hydration enthalpy[106]. Charged head groups can also be classified as kosmotrope and chaotrope, and LMWA can be applied to ion-charged site interactions[108]. A schematic of LMWA is given in Figure 3.15.

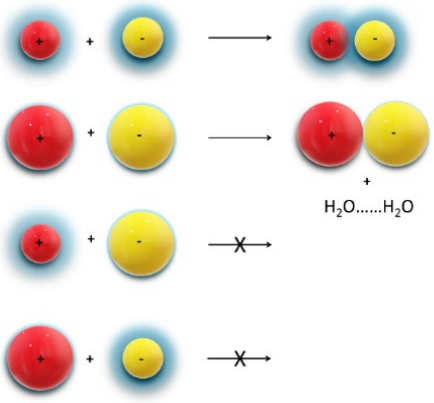

Figure 3.15 Schematics of LMWA: a kosmotropic (chaotropic) cation would form a contact ion pair with a kosmotropic (chaotropic) anion, whereas a kosmotropic (chaotropic) cation would not form a contact ion pair with a chaotropic (kosmotropic) anion.

3.7.2 Dispersion interactions

Our previous discussions of specific ionic effects focused on electrostatics and hydration. Ninham and colleagues hypothesized that dispersion forces could be the source of specific interactions[97]. In addition to the electrostatic image forces, ions undergo a quantum mechanical fluctuation and experience a dispersion potential at every charged substrate/water interface, as predicted by Lifshitz theory[109]. To account for this an additional mean field term ($U_i^{dispersion}$) has added to conventional Poisson Boltzmann equation.

The dispersion potential is given by the following equation

$$U_{\pm}(x) = \frac{1}{x^3}\int_0^{\infty} \frac{\alpha(i\omega)}{\varepsilon_w(i\varepsilon)}\left(\frac{\varepsilon_w(i\omega)-\varepsilon_s(i\omega)}{\varepsilon_w(i\omega)+\varepsilon_s(i\omega)}\right) d\omega \qquad (7)$$

where α(iω) is the dynamic polarizability of the ions as a function of frequency (ω), x is the distance between the ion and the interface, and $\varepsilon_w(i\omega)$ and $\varepsilon_s(i\omega)$ are the dielectric functions of water and of the substrate. This equation indicates that the dispersion interaction is ion and surface dependent, may act in the same direction for both anion and cation. Whereas the electrostatic interactions of surface on cation and anion always goes in the opposite direction. The dispersion forces can even drive the adsorption of anions at a negatively charged interfaces[96] (see Figure 3.16), thus play a substantial role in several ion specific phenomenon[102].

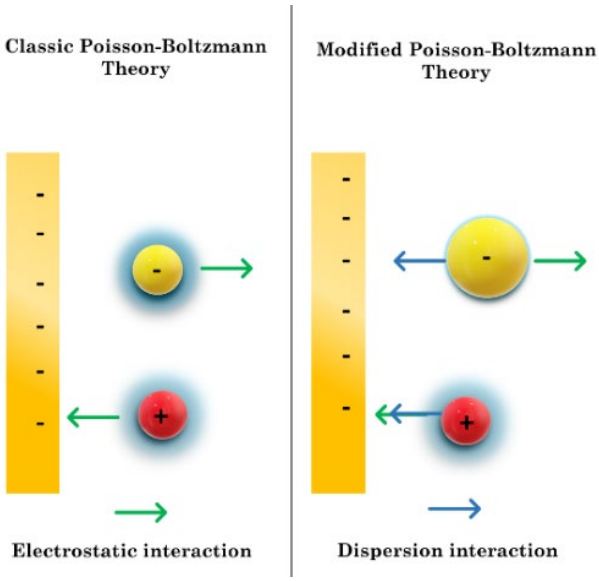

Figure 3.16 Schematic representation of the classic Poisson–Boltzmann theory and its modification that includes ion dispersion forces.

3.7.3 Benselfelt's semi-quantitative model

Ions specific effects have shown to be important in cellulose systems, especially in cellulose self assembly[110,111]. Benselfelt et al.[111] formulated a semi-quantitative model to explain multivalent ion-induced cellulose nanomaterials interactions. According to Benselfelt et al.[111], the principal mechanism involved in ion-induced interactions are:

1. Ion-ion correlations
2. Dispersion forces
3. Metal-ligand complexation
4. Local acidic environment

Ion-ion correlation is ubiquitous in charged systems. In mean-field descriptions of charged interfaces, we have seen that the charged surfaces are associated with a 'uniformly' distributed counterion cloud. In reality, these counterions could undergo fluctuations due to thermal energy and cause instantaneous dipoles, leading to attractive interactions in colloids. Ion-ion correlations depend mainly on the counterion's valency and charge density of the interacting particle. Hence, it is not regarded as a source for specific ionic effects.

The mechanisms responsible for specific ionic effects are dispersion forces, metal-ligand complexation, and local acidic environment. We have already discussed dispersion interactions in the previous section. The key parameter that influences dispersion interactions is the polarizability of ions. Metal-ligand complexation involves the formation of a co-ordinate bond (dative bond) with the metal ion and charged head groups (ligand). The logarithm of the first association constant for metal-ligand complexation represents the stability of the complex. The following mechanism in the list is the local acidic environment changes. Ions that have a strong affinity towards hydroxyl groups (-OH) can behave like acids when dissolved in water; this results in a local pH reduction of up to 2 at the interface, which is significantly below the isoelectric point of carboxylic groups, causing them to become protonated and thus, potentially increasing interactions between materials.

Chapter 4

Driving force for adsorption of CMC on cellulose

Motivation

The presence of hydroxyl groups and structural similarities of the CMC backbone with cellulose have led researchers to consider that hydrogen bonding and co-crystallizations are responsible for CMC adsorption. Despite many attempts to comprehend the adsorption of negatively charged polymers on cellulose, no conclusive statement regarding the adsorption mechanism has been established. While it is evident that both entropic and enthalpic factors may play a role in adsorption, quantifying these effects requires systematic thermodynamic analyses. Identifying the driving force of the adsorption process would allow the process to be tuned efficiently.

The equilibrium constant obtained from Langmuir adsorption isotherms has often been used to compute thermodynamic parameters of adsorption events. Recently, it has been suggested that a similar strategy can be used for thermodynamic profiling of adsorption of carbohydrate-binding proteins to cellulose surface[112–114]. However, the use of equilibrium constant obtained from Langmuir isotherm for thermodynamic profiling of polymer adsorption events should be considered cautiously according to Latour[115], since the state of equilibrium in polymer adsorption is different from adsorption of small molecules. Moreover, the Langmuir model is only applicable to monolayer adsorption. Because of this reason, in this thesis, an alternative method, isothermal titration calorimetry, has been used to analyse the thermodynamic profile of the adsorption of CMC on cellulose surface. Isothermal titration calorimetry (ITC) is a calorimetric titration technique in which heat change associated with binding events is quantified to compute thermodynamic parameters. Figure 4.1 shows the integrated heats upon injection of the CMC[1*] into CNF suspension. A detailed description of the experimental procedure is included in the Appendix (section 9).

[1*] *A CMC-Na with Mw of 90.5 KDa and DS of 0.7 was used for all adsorption experiments in this thesis.*

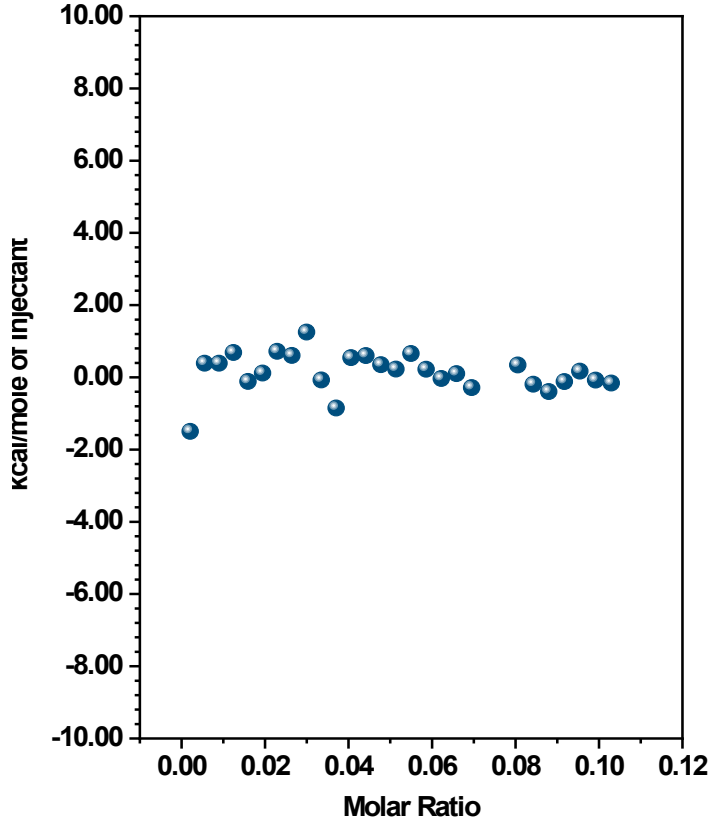

Figure 4.1 Integrated heats upon injection of the CMC solution into CNF suspension (Unpublished ITC experiments performed by Prof. Ali Assifaoui, VA participated in the experiment design).

As seen in Figure 4.1, CMC adsorption does not result in considerable heat change, ruling out the possibility of specific interactions such as hydrogen bonding being involved in the interaction of CMC with the cellulose surface. Given that CMC adsorption on cellulose occurs spontaneously, it must be associated with a negative free energy change. Since the enthalpy change during the adsorption of CMC on cellulose is negligible, a negative free energy change must originate from a positive entropy change. Recently, it has been claimed that hemicellulose adsorption on highly hydrated systems such as cellulose is driven by the entropy gain associated with the release of unfavourably arranged water molecules from the surface[116,117]. Additionally, a similar mechanism for the adsorption of negatively charged PEDOT:PSS on cellulose surface has been proposed[118]. To test this hypothesis in the case of CMC adsorption, we evaluated CMC adsorption from water and deuterated water (D_2O) at an ionic strength of 250 mM $CaCl_2$, where adsorption is likely to be driven by non-electrostatic forces, as predicted by Fleer et al.[67].

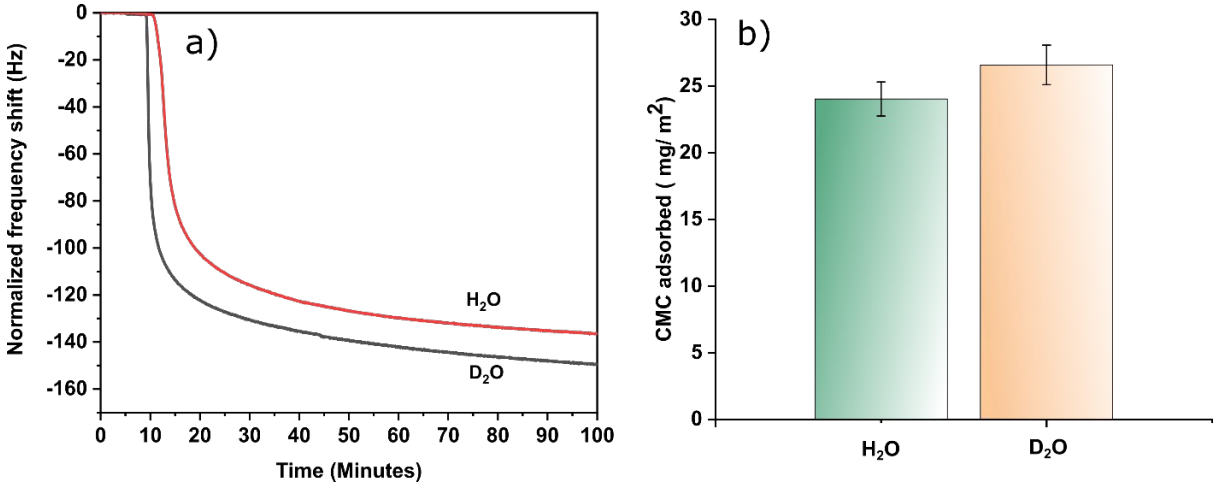

Figure 4.2 a) Representative QCM-D frequency curves of adsorption of CMC on cellulose from D_2O and H_2O. b) Adsorbed CMC calculated using Johannsmann's model.

The observed change in frequency shift implies that CMC adsorption is more favoured from D_2O than H_2O. Thus, although D_2O and H_2O are often considered similar liquids, there is a significant difference in their physicochemical properties stemming from differences in their intermolecular forces. D_2O forms a stronger and higher average number of hydrogen bonds (10%) than normal water[119–121]. Thus, it is a more structured liquid than H_2O[122]. Therefore, when CMC is adsorbed from D_2O, the entropy gain due to the release of structured D_2O molecules from the cellulose surface would be more significant and result in higher adsorption than CMC adsorbed from H_2O, as is seen in Figure 4.2. It has also been suggested that in D_2O, the hydrophobic interactions are more significant[123]. However, since Kargl et.al[52] has observed that the CMC is adsorbing less onto partially acetylated cellulose surface (more hydrophobic) compared to a fully regenerated cellulose surface, the involvement of hydrophobic interactions in CMC adsorption could be of less significance compared to the entropy gain due to the release of structured water.

To further investigate the role of entropy in CMC adsorption, CMC adsorption was carried out at high and ambient temperatures (see Appendix section 8 for experimental details). Figure 4.3 shows representative QCM-D curves for CMC adsorption at different temperatures. The increased frequency shift at 45 ^{0}C demonstrates that CMC adsorption increases as the temperature rises. Laine et.al[41] also reported that increased temperature favoured the adsorption of CMC on cellulose-rich fibers. This observation further strengthens the proposed entropy-driven mechanism[117].

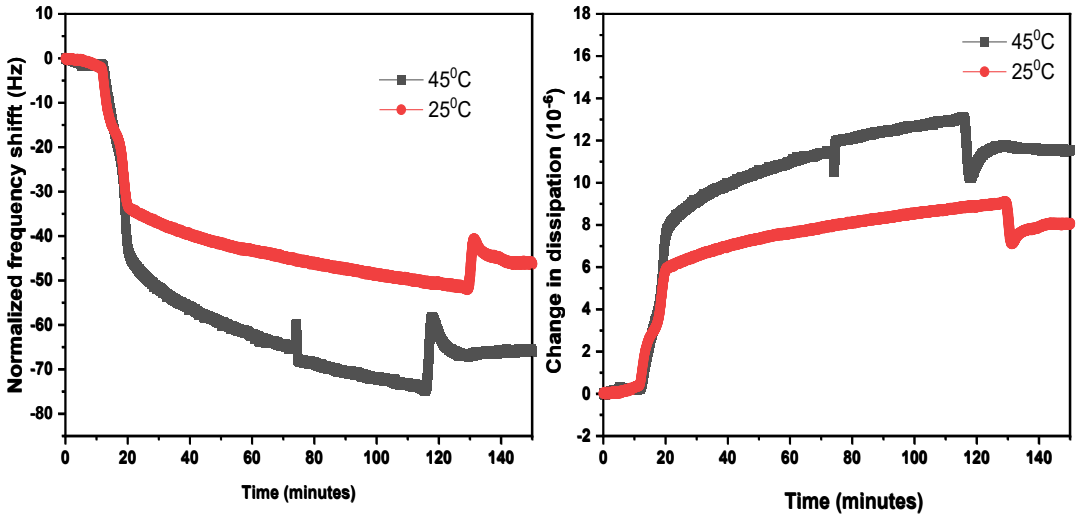

Figure 4.3 A representative QCM-D curve for adsorption of CMC on cellulose from 60 mM NaCl at 25^{0}C and 40^{0}C. (Unpublished and experiments are performed by VA).

Chapter 5

Cation specific effects in CMC adsorption

Motivation

It has been demonstrated that CMC adsorption substantially affects the processing and properties of paper-based products. Therefore, recent efforts have been undertaken to incorporate CMC adsorption into existing pulp producing units to modify fibers in the manufacturing process. Integrating a polymer adsorption step into the paper mill's process is economically viable and complies with green chemistry concepts. Nonetheless, specific considerations must be addressed to achieve the best industrial process possible. One of the primary impediments to introducing CMC adsorption is the use of $CaCl_2$: its use in the Kraft pulping process is undesirable due to scaling issues caused by calcium oxide and calcium carbonate deposition in pipes[124]*. As a result, an industrially viable divalent cationic electrolyte system should be used to modify CMC adsorption on cellulose surfaces. Magnesium is a desirable contender for this purpose, as magnesium salts are already used in the oxygen delignification step of Kraft pulping to prevent degradation and boost yields. Magnesium ions have also been demonstrated to improve the brightness of pulp when used in conjunction with hydrogen peroxide bleaching processes*[125]*.*

In Article 2, cation specific effects in CMC adsorption have been studied. Model system studies have been combined with adsorption studies on cellulose-rich pulp fibers commercially available. Figure 5.1 shows a representative QCM-D curve for adsorption of CMC from 20 mM $CaCl_2$ and 20 mM $MgCl_2$. When solutions containing CMC were injected into the flow cell, an instantaneous decrease in frequency was detected, indicating an increase in the mass at the solid/liquid interface (Figure 5.1).

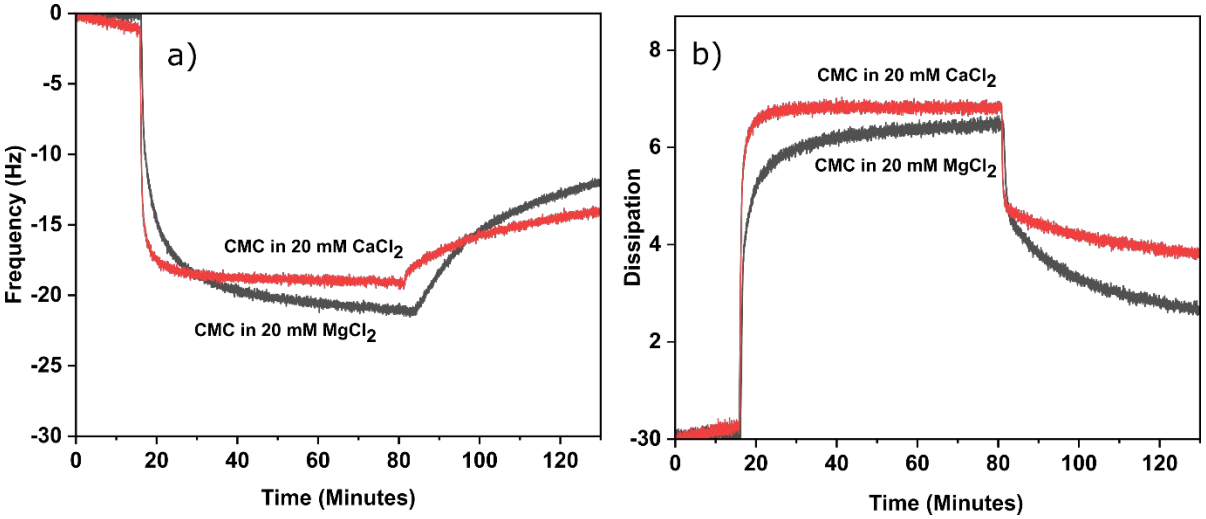

Figure 5.1 Changes in frequency and dissipation over time during the adsorption of CMC on CNF films from solutions containing 20 mM $CaCl_2$ (red curve) and $MgCl_2$ (black curve).

A corresponding increase in dissipation was found in both cases, indicating the adsorbed layers' viscoelastic nature. Similar viscoelastic behaviour has been observed by Liu et al. on adsorption of CMC on regenerated cellulose surfaces in the presence of $CaCl_2$[53]. Rinsing with a similar salt solution increased the frequency, indicating that some loosely bound adsorbed chains desorbed off the surface. Additionally, the data indicate that the adsorbed layer had not reached equilibrium after 50 minutes of rinsing. The calculated aerial mass of adsorbed CMC prior to and the following rinsing is reported in Table 5.1 for both salt solutions. It can be seen that the CMC layer adsorbed with $CaCl_2$ was more stable than the CMC layer adsorbed with $MgCl_2$.

Table 5.1 Amount of CMC adsorbed on CNF calculated using Johannsmann's model[126].

Salt	**Sensed mass (mg/m²)**	
	Prior to rinsing	Post rinsing
$MgCl_2$	4.4 ± 0.2	2.8 ± 0.3
$CaCl_2$	4.2 ± 0.4	3.1 ± 0.1

The differences in adsorption behaviour of CMC in the presence of Mg^{2+} and Ca^{2+} indicate that the adsorption of CMC on cellulose surface is ion specific. CMC was adsorbed on commercially available softwood kraft fibers kindly provided by the Södra Cell to further examine ion-specific adsorption. The total charge of CMC-modified and unmodified cellulose fibers is shown in Figure 5.2.

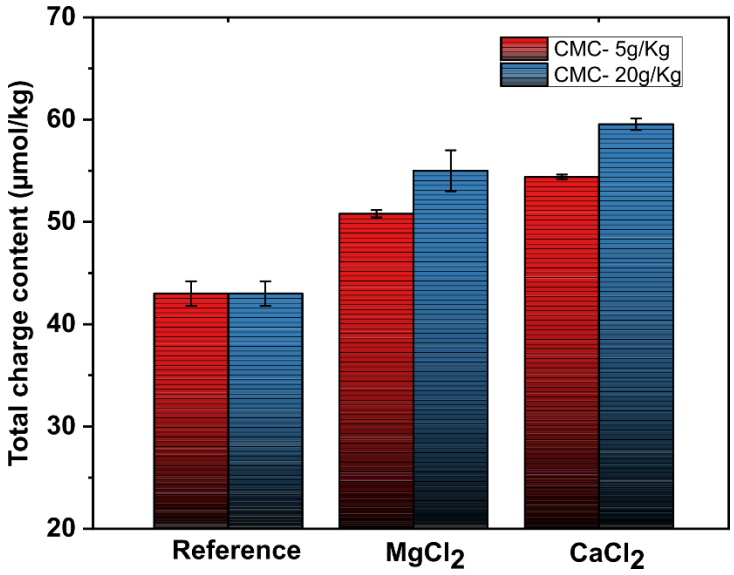

Figure 5.2 Total charge of unmodified cellulose fibers and modified with different amounts of CMC in $CaCl_2$ and $MgCl_2$ environments.

The cellulose-rich fibers treated with CMC in $CaCl_2$ and $MgCl_2$ environments exhibited a higher total charge content compared to the unmodified pulp, indicating that CMC chains are attached to the cellulose surface[41]. The amount of CMC attached was higher in the presence of $CaCl_2$ compared to $MgCl_2$, which confirms the ion-specific nature of CMC adsorption. Results obtained from TOC analysis and anionic content analysis using polyelectrolyte titration were consistent with total charge analysis (Appendix section 7). The data obtained by total charge measurements were used to calculate the amount of CMC attached to the fiber and presented in Table 5.2.

Table 5.2 Total charge and amount of CMC attached on modified fibers in the presence of $CaCl_2$ and $MgCl_2$ at two different CMC loadings.

Salt	**Total charge content (µmol/g)**			**Amount of CMC attached (mg/g)**	
	CMC (0 g/kg)	CMC (5 g/kg)	CMC (20 g/kg)	CMC (5 g/kg)	CMC (20 g/kg)
$MgCl_2$	43	50.9	55.0	2.0	2.9
$CaCl_2$	43	54.1	56.9	3.1	3.6

However, compared with Laine et al.[41] the increase in total charge obtained in this study is lower. This may be due to that the experiments reported by Laine et al.[41] were conducted at higher temperatures and higher salt concentrations, which favour CMC adsorption on cellulose fibers[41]. It should also be noted that the CMC used in this investigation has a low molecular weight and a high degree of substitution (DS), which are known to suppress such adsorption[41].

Table 5.3 Surface charge and increase in total charge of the modified fibers.

Salt	**Surface charge content µmol/g**			**Increase in total charge content µmol/g**		**Percentage of increase in total charge on the surface**	
	CMC (0 g/kg)	CMC (5 g/kg)	CMC (20 g/kg)	CMC (5 g/kg)	CMC (20 g/kg)	CMC (5 g/kg)	CMC (20 g/kg)
$MgCl_2$	4.7	6.1 ± 0.6	8.5 ± 0.1	7.8	12.0	18.1	31.5
$CaCl_2$	4.7	6.3 ± 0.1	8.8 ± 0.1	11.1	13.9	14.6	29.4

Measurements of surface charge indeed supported previous observations that the amount of CMC adsorbed was greater in the presence of $CaCl_2$ than $MgCl_2$ (Table 5.3). However, when the total charge measurements and surface charge measurements are compared, it is evident that the contribution made by the surface charge to the total charge is only 15%, this means that 85% of the charges are located inside the fiber wall. In our studies, the percentage increase in surface charge at higher loadings of CMC (20 g/kg) was about 30%. While, Laine et al.[41] found more than 50% increase in the surface charge content relative to the total charge content. However, the CMC used by Laine et al. had a larger Mw (280 kDa) than the CMC (90 kDa) used in this study: the smaller dimension of CMC allow a larger amount to penetrate the fiber wall, thereby resulting in a lower surface selectivity. The percentage increase in the surface charge of pulp treated with CMC in the presence of $MgCl_2$ was nevertheless slightly higher than for the pulp treated in the presence of $CaCl_2$. The CMC concentration is also found to influence the adsorbed amount of CMC. The increase in CMC concentration in the system resulted in higher CMC adsorption on the cellulose surface. However, from Table 5.2, it can be seen that a fourfold increase in CMC concentration only resulted in a 10% increase in CMC adsorption, suggesting that the adsorption sites are close to saturation even at a CMC concentration of 5 g/kg.

The results obtained from adsorption studies performed on the commercial pulp and the QCM-D studies on model cellulose showed that CMC adsorbs in considerable amounts in the presence of both Mg^{2+} and Ca^{2+}. However, ion specificity was evident from the results. Ion specific effects have been previously reported in the interactions of materials containing carboxylate groups ($-COO^-$), properties such as gelation rheological and mechanical properties were reported to be influenced by identity of ions present in the system[127–130]. For example, the gel strength of polygalactoglucoronate was higher when cross-linked with Ca^{2+} ions than with Mg^{2+} ions[128]. These changes are often assigned to the formation of metal-ligand complexes. The stability of metal-ligand complexes is typically represented by the stability constant, which is defined as the logarithm of the first association constant k_1 [131]. Often, there is an insufficient correlation between the metal complex's stability constant and the observed property changes. For example, Ca^{2+} interacts more strongly with the carboxyl group than Mg^{2+} does when these groups are present in polyelectrolytes such as alginate or pectin[132,133]. However, Hancock and Marsicano demonstrated that ($-COOMg^+$) complexes' stability constant is greater than ($-COOCa^+$) complexes, indicating that the metal-ligand complexation might not be a dominant interaction mechanism.

A semi-quantitative model presented by Benselfet et al.[111] was employed to gain a mechanistic understanding of the ion-specific effect on CMC adsorption. This model was first designed to describe the interactions of multivalent ions in charged cellulose nanoparticles. Ion-ion correlation and dispersion interactions are relevant in the case of our system. However, the involvement of metal-ligand complexation and local acidic environment change can be neglected because of small values for association constants.

Two plausible mechanisms that could be involved in ion-induced interactions in CMC adsorptions on cellulose are:

- Ion-ion correlations among CMC chains and between CMC chains the cellulose surface, induced by the divalent ions.
- Dispersion interactions among CMC chains (Figure 5.3a) and between CMC chains the cellulose surface, induced by the divalent ions (Figure 5.3b).

The charge density of the interacting materials and the valency of the counterions determine the ion-ion correlation interactions. Both ions utilized in this investigation are divalent; consequently, the interactions generated by ion-ion correlation should be identical in both situations and cannot account for the observed variation in the amount adsorbed.

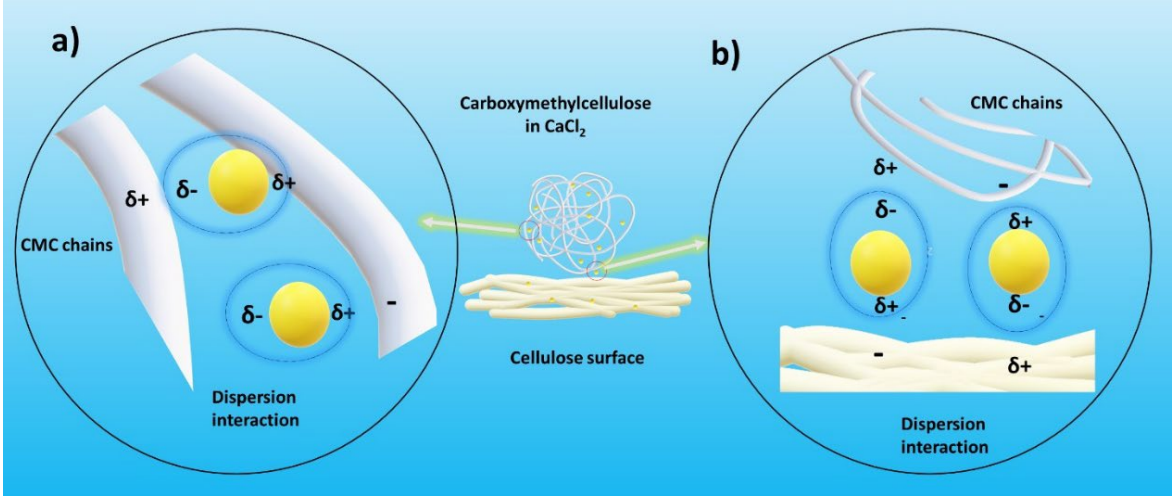

Figure 5.3 Dispersion interactions induced by Ca^{2+} ions between a) CMC chains in solution and b) CMC chains and a cellulose surface.

The most evident distinction between Ca^{2+} and Mg^{2+} is the ion size: Ca^{2+} ions are approximately 30% bigger, which results in a greater polarizability[134]. The polarizability of ions has been associated with dispersion interactions[135], which are induced by the introduction of local perturbations in the electron cloud of the ions, resulting in the development of induced dipoles. The induced dipoles in the electron cloud surrounding the ions can interact with the permanent or induced dipoles in the polyelectrolyte chains and cellulose surfaces, resulting in interactions between the polyelectrolyte chains and between polyelectrolyte chains and the cellulose surface. The greater polarizability of Ca^{2+} ions means that they can induce stronger dispersion interactions than Mg^{2+} ions.

The solutions of CMC in the presence of Mg^{2+} and Ca^{2+} were analysed using dynamic light scattering. It was observed that in the presence of divalent ions, the hydrodynamic diameter of the CMC (CMC in Ca^{2+} - 5 nm and CMC in Mg^{2+} - 3.5 nm) has been reduced compared to the hydrodynamic diameter of CMC in the same concentration of NaCl (9.7 nm) suggesting that in the presence of divalent ions the CMC chains are less expanded in water. However, when comparing the hydrodynamic diameter of CMCs in the presence of Ca^{2+} and Mg^{2+}, CMC hydrodynamic diameter is higher in the presence of $Ca^{2+,}$ suggesting that Ca^{2+} ions promote the multichain association of CMC (Figure 5.3a). Sharratt et.al[136] observed that in the presence of Ca^{2+} ions, CMCs form aggregates of size ranging from 20-40 nm, which supports the multichain association. The changes in CMC solution structure could be a reason for the source for the observed specific ionic effects in CMC adsorption. In addition, the possibility of having increased interaction between CMC and cellulose through dispersion interactions (Figure 5.3b) should not be neglected.

Chapter 6

Distinguishing the effect of cations

Motivation

We have seen in the previous chapter that the identity of the divalent ions influences the adsorption of CMC. It is well known that polymer adsorption is a multifaceted process that involves a polymer solution (liquid phase) and a surface immersed in it, where characteristics of both the solution and the surface can affect the adsorption processes. Divalent ions have the potential to alter both the solution's properties and the surface's properties. However, which of these changes has the dominant role in steering the adsorption process?

In this chapter, the aforementioned question has addressed by studying the changes in the properties of the CMC solution and cellulose surface in different ionic strengths of $CaCl_2$ and then correlated it to the adsorption.

6.1 CMC solution in different ionic strengths of $CaCl_2$

We discussed the change observed in the hydrodynamic diameter of CMC in Ca^{2+} and Mg^{2+} in the previous chapter. The result indicated a multichain association of CMC chains in the presence of Ca^{2+} ions. To investigate this further, the evolution of the hydrodynamic sizes of the CMC chains with an increase in ionic strength of $CaCl_2$ (5 mM to 250 mM) were probed using dynamic light scattering. The intensity particle size distribution (PSD) (red curve in Figure 6.1a) is the primary PSD obtained from the light scattering experiment, indicating that most of the CMCs have a hydrodynamic diameter greater than 100 nm. In contrast, the volume PSD of the same sample demonstrates a single sharp peak, showing that the majority of the CMC volume has a hydrodynamic diameter of less than 5 nm (blue curve in Figure 6.1a). The discrepancy in the hydrodynamic diameter between the intensity PSD and volume PSD of the same solution is related to the method adopted to extract the hydrodynamic diameter from the autocorrelation function. The intensity PSD is calculated simply based on the light scattered by the solution. Larger particles dominate scattering and have a more significant effect on the particle size distribution. Mie theory was utilized to calculate volume PSD, which takes into account optical parameters such as refractive index and light absorption by the material into account and scattered intensity[137]. The volume PSD will be used exclusively in the discussion going forward, as this is the appropriate way for reporting hydrodynamic size.

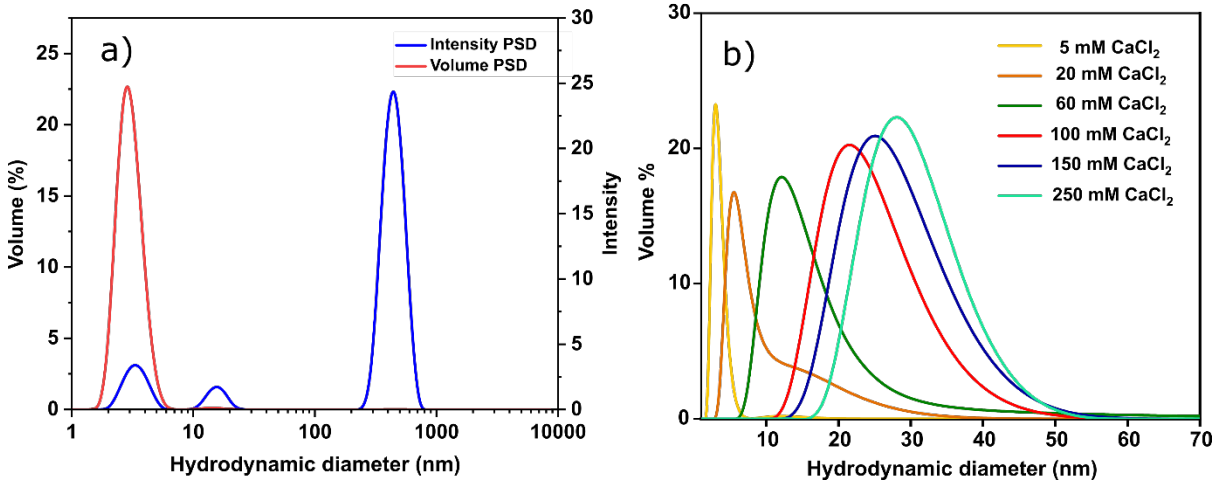

Figure 6.1 a) Volume (red) and intensity (blue) PSD of CMC in 5 mM $CaCl_2$.
b) Volume PSDs of CMC for different ionic strengths of $CaCl_2$.

Figure 6.1b represents the volume PSD of CMC solutions in 5-250 mM concentration of $CaCl_2$. The increase in the concentration of Ca^{2+} ions in the solutions resulted in a larger average size and broader size distributions. The average size obtained from the volume PSD is plotted as a function of $CaCl_2$ concentration (Figure 6.2a).

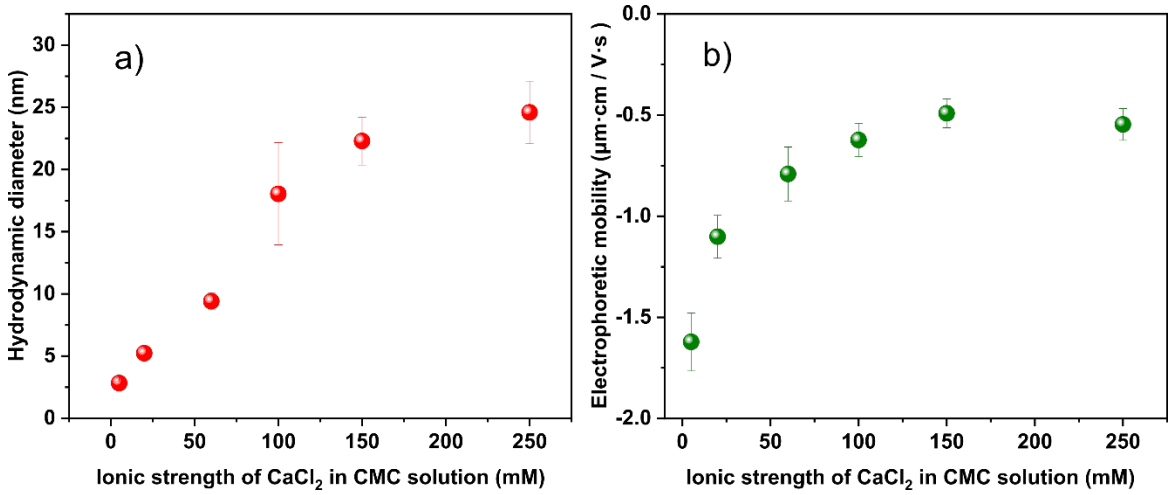

Figure 6.2 a) Average hydrodynamic diameter obtained from the volume PSD and b) the electrophoretic mobility of CMC solutions for different ionic strengths of $CaCl_2$.

From 5 to 100 mM $CaCl_2$, a linear increase in hydrodynamic size can be observed. After 100 mM, the curve flattens out, and the average hydrodynamic diameter was around 25 nm at 250 mM $CaCl_2$. This is consistent with the observation by Sharratt et al.[136].

The rationale for the observed trend in the hydrodynamic diameter is due to Ca^{2+} ions interaction with the CMC polymer chains. As discussed in Chapter 5, Ca^{2+}

ions can interact with CMC chains via ion-ion correlations and dispersion interactions[138]. This may result in a decrease in the charge density of CMCs as demonstrated by the electrophoretic mobility experiments illustrated in Figure 6.2b. Electrophoretic mobility increased with increasing $CaCl_2$ concentrations and reached a plateau at 60 mM. Reduced charge on the CMC chains promotes inter- and intra-chain association and the creation of multichain clusters, resulting in the observed trend for the hydrodynamic diameter of the CMC at various $CaCl_2$ concentrations.

6.2 CNF suspensions in different ionic strengths of $CaCl_2$

The effect of $CaCl_2$ concentration on the surface of cellulose was studied by measuring the zeta potential of CNF suspensions in different ionic strengths of $CaCl_2$ (Figure 6.3). This experiment should have been conducted on CNF-coated QCM-D sensors; instead, it was conducted on CNF suspensions due to the experimental constraints. There is a possibility of structural reconfiguration of CNF suspensions in the presence of divalent cations. Valencia et al. reported that divalent ions induce reversible changes in the microstructure of TEMPO-oxidized CNF suspensions[139]. Similar reorganization of the CNF microstructure generated by cations within a film may be more limited than seen for dispersions.

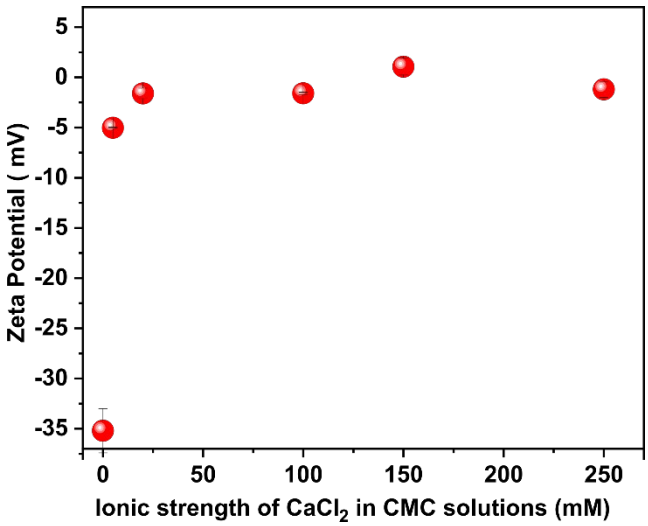

Figure 6.3 Zeta potential of CNF suspensions in different ionic strengths of $CaCl_2$.

CNF suspension in the absence of $CaCl_2$ showed a zeta potential of -35 mV, indicating that the CNF surface was negatively charged, and the dispersion was colloidally stable. However, in the presence of a minimal amount of $CaCl_2$ (5 mM), the colloidal stability of the suspension has been lost. Because the CNF suspensions were not colloidally stable in all the concentrations of $CaCl_2$ utilized,

the zeta potential values provided in Figure 6.3 should only be considered qualitative in the following discussions. However, the tampered colloidal stability of CNF suspension in the presence of $CaCl_2$ indicates that the charges are screened.

6.3 Adsorption of CMC from $CaCl_2$ solutions

We have seen how the CMC chains and the CNF surface behave in the presence of different ionic strengths of $CaCl_2$. Figure 6.4 shows representative QCM frequency and dissipation curves for CMC adsorption in the presence of $CaCl_2$.

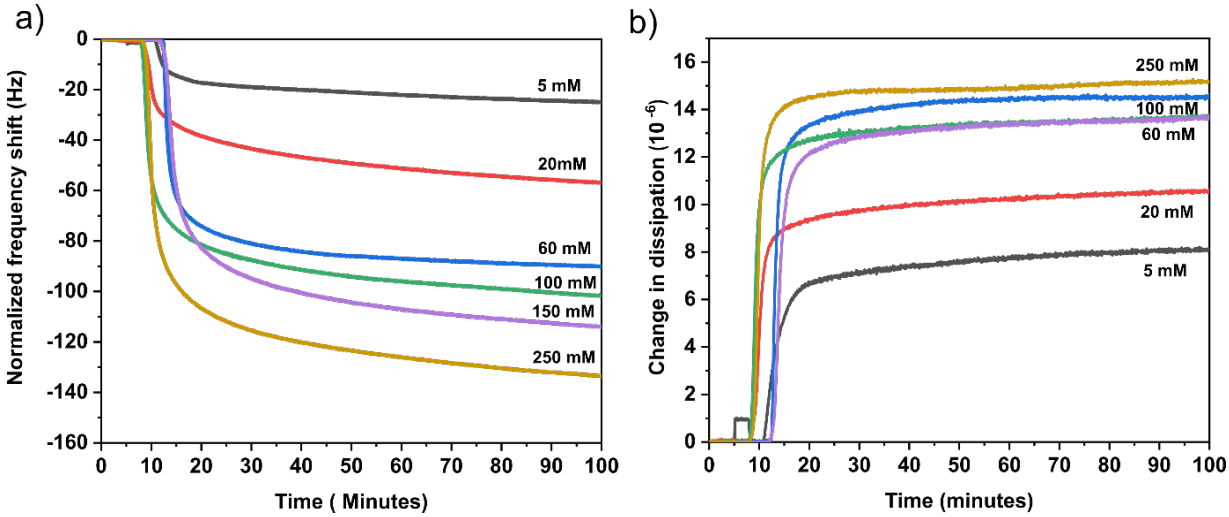

Figure 6.4 Representative a) frequency (3rd overtone) and b) dissipation curves for the adsorption of CMC on CNF model surfaces in aqueous $CaCl_2$ environments.

These adsorption curves can be used to generate the following general conclusions: To begin, adsorption of CMCs onto the CNF model film is slow at all $CaCl_2$ ionic strength investigated, with no plateau occurring even after 90 minutes. The frequency shift and dissipation shift increase as $CaCl_2$ ionic strength increases, demonstrating that $CaCl_2$ significantly affects the CMC adsorption process. This is congruent with the findings of Laine et al. [41] and Liu et al. [53], who examined CMC adsorption onto cellulose-rich macrofibers and regenerated cellulose surfaces, respectively. The adsorbed CMC per unit area is plotted versus the $CaCl_2$ concentration using Johannsmann's model, as illustrated in Figure 6.5.

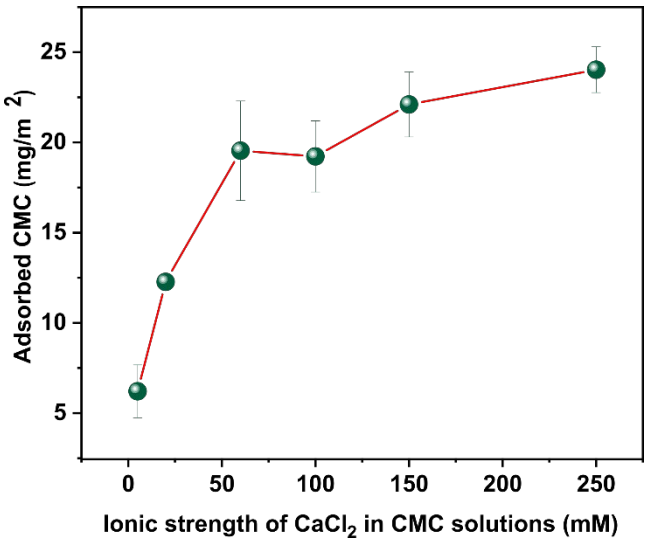

Figure 6.5 The mass of the adsorbed CMC per unit area on a cellulose surface from CMC solutions with different concentrations of $CaCl_2$.

From Figure 6.5, it can be seen that the adsorption increased as the ionic strength of $CaCl_2$ increases. The adsorbed CMC increased significantly from 5 to 60 mM $CaCl_2$ and started to level off. The adsorption isotherm depicted in Figure 6.5 resembles the curve anticipated by S-F theory for the specific situation of anionic polyelectrolytes adsorbing on a like-charged surface. According to S-F theory, at larger salt concentrations, the charges in both the polyelectrolytes and the surface are screened (i.e., q_m and σ_0), and non-electrostatic forces purely regulate adsorption. Notably, S-F theory examines only monovalent salts. However, a comparison of the ability of divalent and monovalent ions to increase the amount of adsorbed at the same ionic strength indicates that, aside from the apparent electrostatic screening effects, divalent metal ions contribute favourably to the adsorption process[41,53]. This positive effect of multivalent ions on adsorption may be due to the structural changes caused in polymer solutions by multivalent ions.

To get further insights on this, the data obtained from the dynamic light scattering of CMC solution is correlated with the adsorption data. Figure 6.6 illustrates the relationship between adsorbed CMC and the electrophoretic mobility and structural characteristics of CMC in the presence of $CaCl_2$.

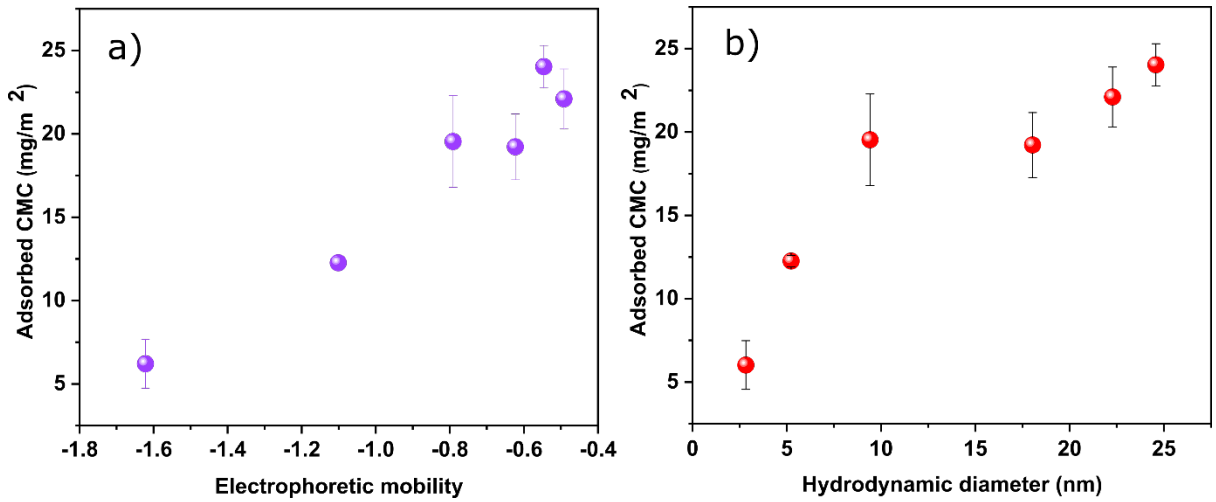

Figure 6.6 a) The adsorbed CMC per unit area at different ionic strengths of $CaCl_2$ plotted against electrophoretic mobility. b) The hydrodynamic dynamic diameter at a corresponding concentration of $CaCl_2$.

Increases in electrophoretic mobility and hydrodynamic diameter enhance the adsorbed CMC adsorbed per unit area on cellulose. When the data in Figures 6.3 and 6.6 are combined, no such correlation between the zeta potential of the CNF surface and the adsorbed CMC can be found. The obtained zeta potential values indicate that the charge on the surface becomes close to neutral even at a concentration of 10 mM. Additional increase in ionic strength had no discernible effect on the CNF's surface charge. However, the CMC adsorbed per unit area increased with increasing ionic strength up to 250 mM, indicating that Ca^{2+} ions had a significant effect on the solutions side, contributing to adsorption. This explains why the amount of CMC adsorbed correlates with the hydrodynamic size. Additionally, screening the negative charges and multichain association of CMC in the presence of $CaCl_2$ lowers the polymer-solvent interaction, which may contribute to the adsorption driving force.

Chapter 7

Conformations of adsorbed CMC layers

Motivation

The adsorbed polymer chains can take different conformations depending on the adsorbing conditions. Real-time monitoring of changes in adsorbed layer conformation could give insights into the mechanism of the adsorption process. The adsorbed layer conformation is also essential when it comes to final applications. The layer conformation can affect the interaction of the adsorbed polymer layer with other entities such as enzymes and proteins. It has been shown that the adsorbed CMC could increase the wet adhesion between the surfaces through the interdigitation process. In this regard, the conformation of the adsorbed layer should be studied.

The information obtained from QCM-D measurements can be used to get insights on conformational change during the adsorption process. For example, the dissipation changes corresponding to frequency shift can be represented in Figure 7.1, typically known as the dissipation-frequency plot (D-f plot).

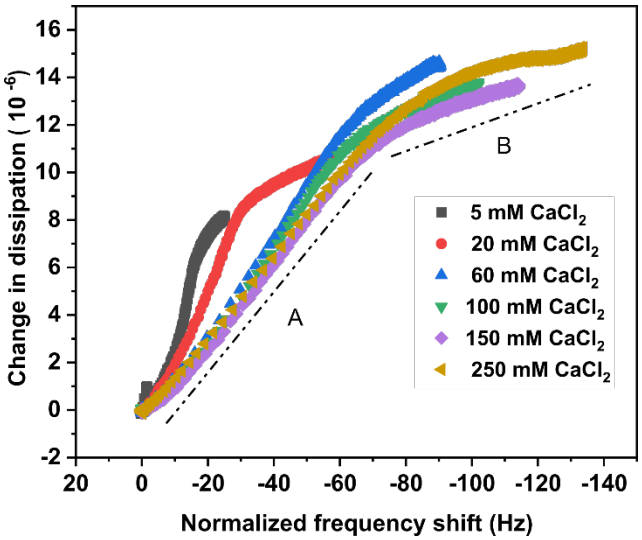

Figure 7.1 Change in dissipation as a function of normalized frequency shift (3rd overtone) during the adsorption of CMC on CNF model surfaces in aqueous $CaCl_2$ environments.

CMC adsorption D-f plots exhibit a continuous curve at all $CaCl_2$ ionic strengths examined, confirming that CMC adsorption is a slow process. At lower $CaCl_2$ concentrations, the slope of the D-f curves increases, indicating that the adsorbed

layer is more viscous, as demonstrated by the rise in dissipation. On the other hand, increasing the $CaCl_2$ concentration decreases the slope and hence the viscous component, indicating the formation of a denser adsorbed CMC layer.

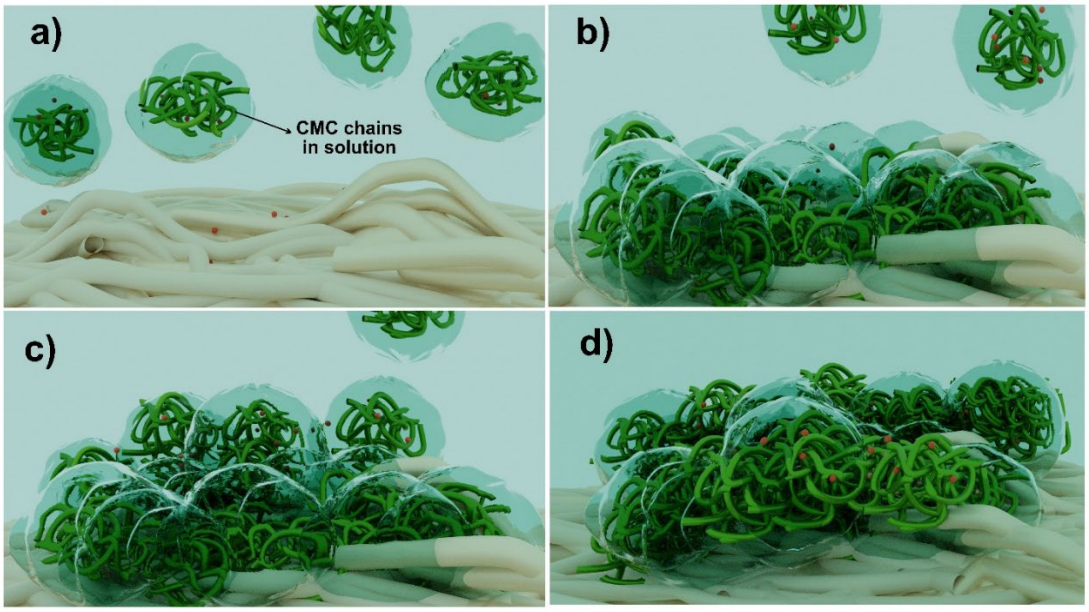

Figure 7.2 Schematic representation of CMC adsorption in the presence of $CaCl_2$ (orange dots). a) CMC chains (green) approach the surface, b) collapse and spread of CMC chains on the cellulose surface and into the pores of the CNF film, c) dangling CMC chains interact with adsorbed CMC on the cellulose surface (2^{nd} stage) and desorption of shorter chains, d) dangling CMC chains penetrate the adsorbed CMC network to form a thicker adsorbed layer.

The degree to which the polymer structure collapses during adsorption is dependent on the polymer's conformation in solution (Figure 7.2a) and the strength of the polymer's contact with the surface. The denser layer generated at higher $CaCl_2$ concentrations suggests that the structure of polymer molecules in contact with the surface collapses (Figure 7.2b), implying favourable interactions between the CMC and the cellulose surface. Adsorption of neighbouring molecules may impede the conformational rearrangement and spread across the surface kinetically. As a result, some adsorbed CMC may be uninvolved in the immediate interaction with the cellulose surface (Figure 7.2c), increasing the layer's viscosity and dissipation. The slopes of the D-f curves (Figure 7.1) altered as adsorption progressed, indicating that the structure of the adsorbed CMC layer changed throughout adsorption. Köhnke et al. made similar observations with the adsorption of arabinoxylans on cellulose[140]. The decreased slope of region B in the D-f plot (Figure 7.1) suggests that the dangling CMC layers diffuse towards the surface and change the adsorbed layer, thereby increasing its density. It could also be caused by conformational changes in the adsorbed layer as a result of the thermodynamically preferred exchange of shorter adsorbed

chains for longer CMC chains. It is possible that Ca^{2+} ions can still induce multichain association on the surface, and, at this stage, the adsorbed layer can be considered a Ca^{2+} cross-linked gel network attached to the cellulose surface.

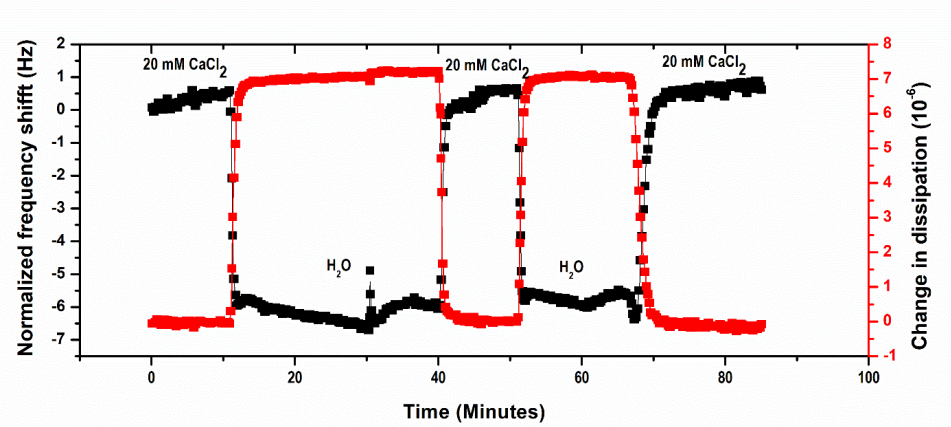

Figure 7.3 Swelling and deswelling cycles of adsorbed layers of CMC (from 20 mM $CaCl_2$) on a cellulose surface.

Figure 7.3 illustrates the swelling and deswelling behaviour of the adsorbed CMC layers in the presence of deionized water and 20 mM $CaCl_2$. The frequency immediately decreases when the 20 mM $CaCl_2$ is replaced with deionized water. This corresponds to water intake, which can also be referred to as swelling of the adsorbed layer. Additional 20 mM $CaCl_2$ injections into the flow cell at 40 and 68 minutes increased the frequency, indicating that the CMC layer deswells or collapses in the presence of Ca^{2+}. Kargl et al[52]. showed similar increases in frequency following water injection into CMC adsorbed film. The swelling-deswelling behaviour was reversible, as demonstrated by two cycles in Figure 7.3, confirming the gel network nature of the adsorbed layers. Similar swelling and deswelling experiments were performed on a CMC layer adsorbed from 20 mM NaCl and presented in Figure 7.4.

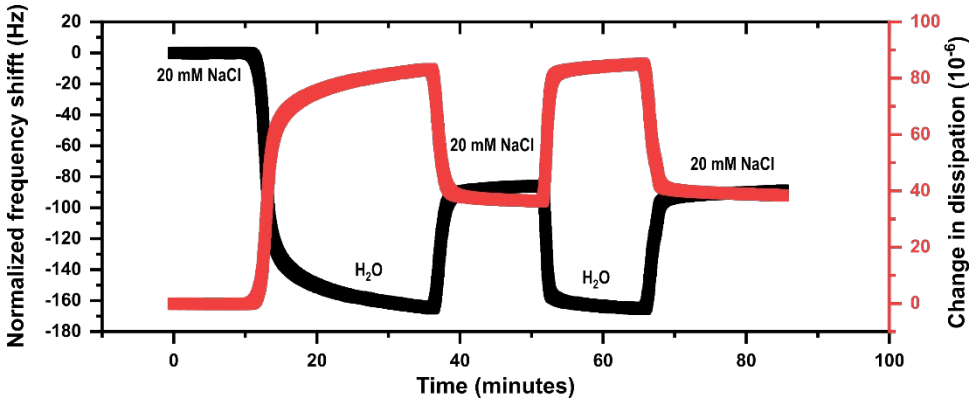

Figure 7.4 Swelling and deswelling cycles of adsorbed layers of CMC from (20 mM NaCl) on a cellulose surface. (Unpublished results experiment performed by VA).

Experiments with a CMC layer adsorbed with 20 mM NaCl have been carried out similarly to the ones described above. However, because of the considerable shift in frequency caused by the injection of water into the QCM-D cell, it can be inferred that the CMC layer adsorbed from NaCl took up a significant amount of water when compared to the CMC layer adsorbed from $CaCl_2$. This demonstrates that the adsorbed layer conformation differs when CMC is adsorbed from NaCl and $CaCl_2$.

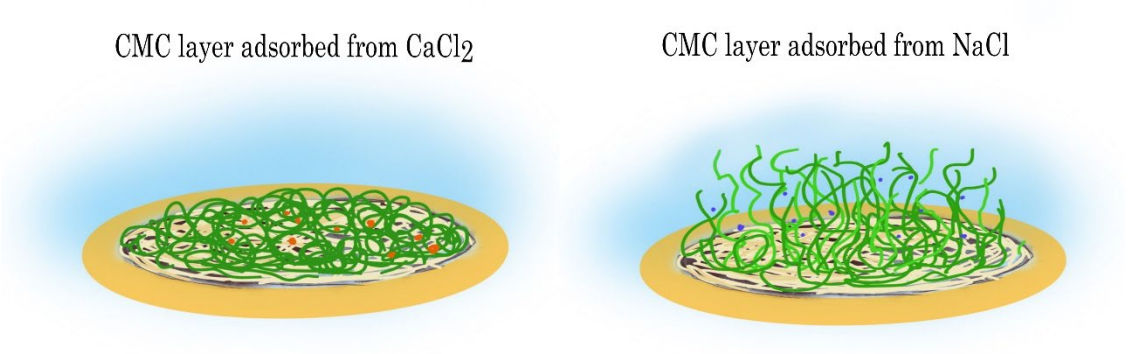

Figure 7.5 Adsorbed layer conformation of CMC adsorbed from $CaCl_2$ and NaCl.

Furthermore, the first swelling and deswelling cycle of the CMC layer adsorbed from NaCl was different from that of the CMC layer adsorbed from $CaCl_2$. Therefore, the partially irreversible behaviour in swelling-deswelling of the CMC layer adsorbed from NaCl could be due to the fact that the CMC layer, when adsorbed from NaCl, might be kinetically trapped and the swelling in water permitted reorganization into a more thermodynamically stable conformation.

Chapter 8

Anion specific adsorption of carboxymethyl cellulose on cellulose

Motivation

We saw in Chapter 5 that Mg^{2+} ions could enhance CMC adsorption. It is, however, less efficient than Ca^{2+}. Magnesium sulfates are added to the bleaching system on purpose to minimize unintended radical reactions. If CMC adsorption is anion specific, we may substitute an appropriate magnesium-anion combination for magnesium sulfate and get improved CMC adsorption and reduced radical reactions.

The anion specific effect on the cellulose surface has initially tested by carrying out zeta potential measurements on cellulose nanofiber suspensions at 0.02 M solutions of magnesium salts containing chloride, bromide, nitrate and sulfate. The CNF suspension, when no salts were added, had a zeta potential value of 35 mV, meaning that the suspension is colloidally stable. Figure 8.1 shows the zeta potential values of CNF suspensions in magnesium salts solutions with different co-ions.

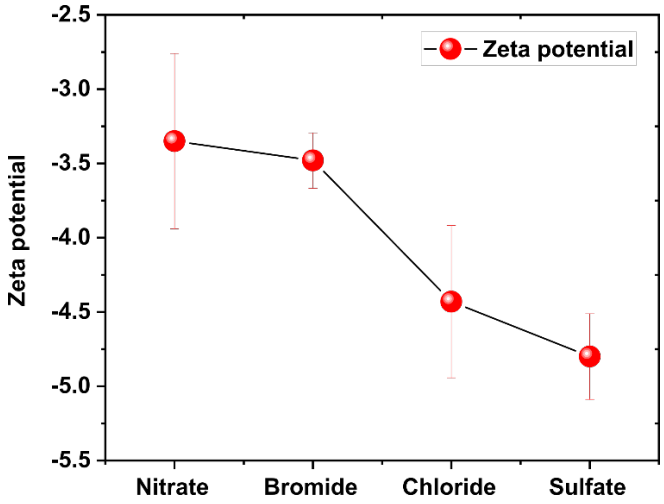

Figure 8.1. Zeta potential of CNF suspension in magnesium salts containing different co-ions.

The addition of salt shifted the zeta potential to a less negative value, meaning that the charges are screened. Interestingly, the zeta potential values of CNF showed changes depending on the co-ion. The difference in zeta potential values of CNF in the presence of magnesium sulfate and nitrate was more significant. A recent investigation by Simonsson et al.[141] also reports a similar trend in

zeta potentials of silica particles in the presence of sodium salt containing sulfate and nitrate. The silica particles had a larger negative zeta potential in the presence of sulfate co-anion than nitrate co-anion. Our results presented in Figure 8.1 indicate that the co-anion identity influences the surface charge of CNF. However, the colloidal stability of the CNF suspension has tampered at 0.02 M concentration of salts, and a quantitatively accurate judgement about co-ion specificity cannot be made based on the zeta potential results.

To understand the anion specific effect on CMC adsorption on cellulose, adsorption was performed using four magnesium salts with different co-ions. Figure 8.2 shows adsorbed mass of CMCs in the presence of 0.02 M of magnesium salts. The adsorbed mass of CMCs was computed using Johannsmann's model.

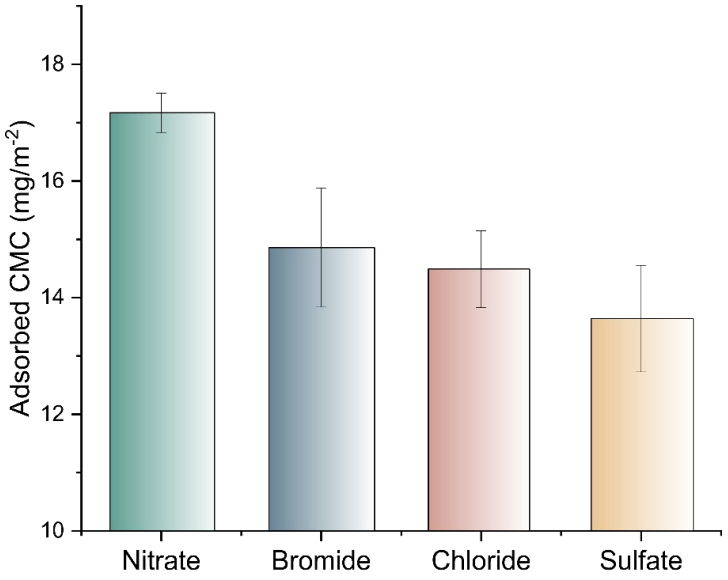

Figure 8.2 Adsorbed mass of CMC from 0.02 M solutions of magnesium salts with different co-ions.

From Figure 8.2, it is evident that when we changed co-anions, the CMC adsorption has also changed. Especially, when adsorption from CMC solutions containing magnesium nitrate and magnesium sulfate was compared, the difference was more pronounced. To investigate this further, CMC adsorption was carried out with different magnesium nitrate and magnesium sulfate concentrations. Figure 8.3a shows adsorbed CMC from different magnesium nitrate and magnesium sulfate concentrations.

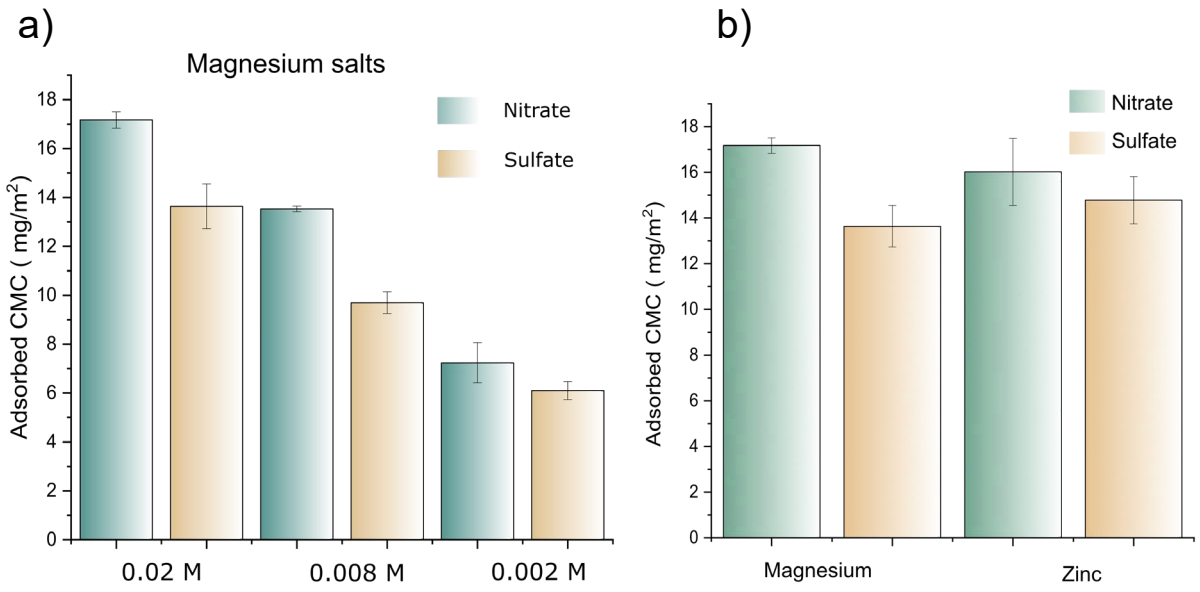

Figure 8.3. a) Adsorbed CMC from different concentrations of magnesium nitrate and magnesium sulfate. b) CMC adsorbed from nitrate and sulfates of magnesium and zinc cations at a concentration of 0.02 M.

As illustrated in Figure 8.3a, CMC adsorption is higher in the presence of magnesium nitrate than in the presence of magnesium sulfate at all concentrations examined. From these observations it is evident that CMC adsorption is prone to anion specific effects.

To investigate the effect of cations on the anion specific character of CMC adsorption, similar adsorption studies were conducted in the presence of zinc cation sulfate and nitrates at a concentration of 0.02 M. Figure 8.3b shows the adsorbed CMCs in the presence of sulfate and nitrates of magnesium and zinc cations. Zinc salts are also showing the same trend as we have seen in the case of magnesium salts. However, the difference is not pronounced as in magnesium salts, meaning that the occurrence of co-ion specificity depends on the cation present in the system.

Generally, ion-specific effects have been ascribed to the ions' hydration. The Jones-Dole viscosity coefficient (B) and hydration enthalpy are two parameters that indicate how well ions are hydrated. The results on CMC adsorption obtained from QCM-D investigations were correlated with the Jones-Dole coefficient and the enthalpy of hydration of co-anions and are shown in Figure 8.4.

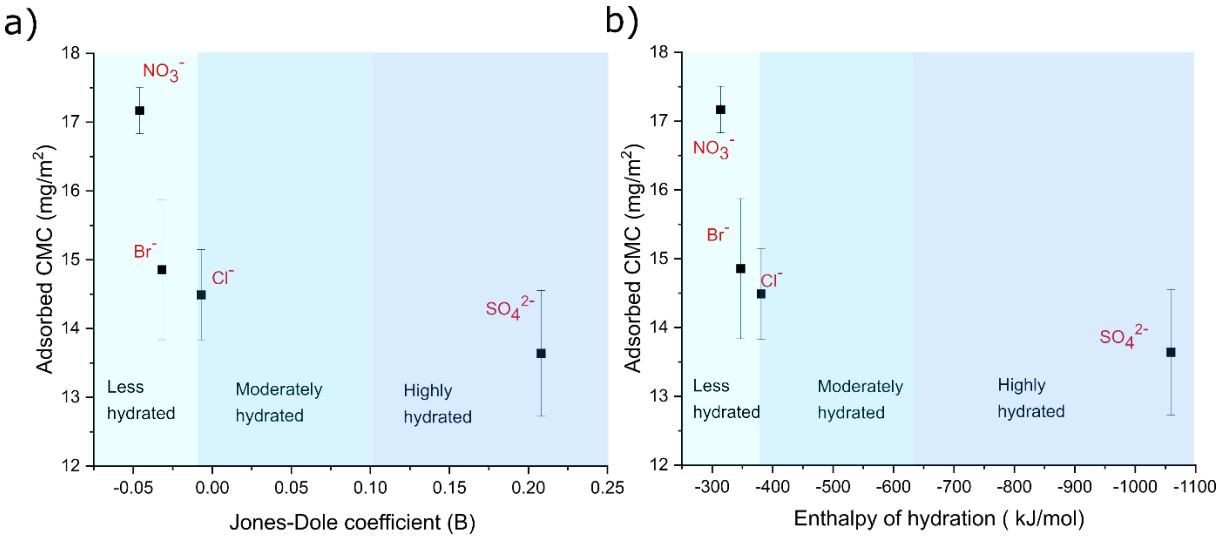

Figure 8.4 a) Relationship between the adsorbed CMC and the hydration enthalpy of co-anion, b) relationship between the adsorbed CMC and the Jones-Dole coefficient of co-anion. The values for Jones-Dole coefficient and hydration enthalpy of ions were taken from Robinsson *et al.*[142] and Smith[143], respectively.

According to Ninham et al., ion hydration dictates how ions are excluded from or included in the interface[94]. The adsorbed CMC in the presence of different ions has been correlated to the enthalpy of hydration and the Jones-Dole coefficient of corresponding anions. As illustrated in Figure 8.4, a clear link exists between the adsorbed CMC and the degree of hydration of co-anions. Adsorption is promoted in the presence of a less hydrated (chaotropic) nitrate ion, whereas adsorption is reduced in the presence of highly hydrated sulfate ions. To elucidate the role of ion hydration in ion selectivity of CMC adsorption on cellulose, the surface properties and hydration characteristics of CNF must be defined. According to Mittal et al.[110], the CNF surface should be considered chaotropic because kosmotropic polymers are water-soluble. The majority of carbohydrate polymers have a positive χ parameter in water, which means that their interactions with water are often weaker than those between water molecules[144]. Additionally, while cellulose's surface is often regarded hydrophilic, its amphiphilic nature has been discussed and concluded to be the reason for cellulose's insoluble nature in water[145]. Although the presence of surface charges on cellulose increases its contact with the solvent, the surface charge density of the CNF used in this study is low (31 µmol/g), and these charges will be screened in the presence of salts, further reducing interactions with water.

According to classical mean-field theories, the anions are expected to exclude from a negatively charged interface. However, investigations suggest that the anions can be adsorbed onto negatively charged interfaces regardless of expected electrostatic repulsion[146–149].

It has been hypothesized that chaotropic ions prefer proximity to a chaotropic surface in order to minimize perturbation of the water hydrogen bonding network, whereas kosmotropic ions avoid proximity to the chaotropic surface and prefer to remain in bulk[110]. Thus, the nitrate ions may preferentially accumulate near the chaotropic CNF surface. The distribution of the chaotropic nitrate ion and the kosmotropic sulfate ion at the interface is depicted in Figure 8.5.

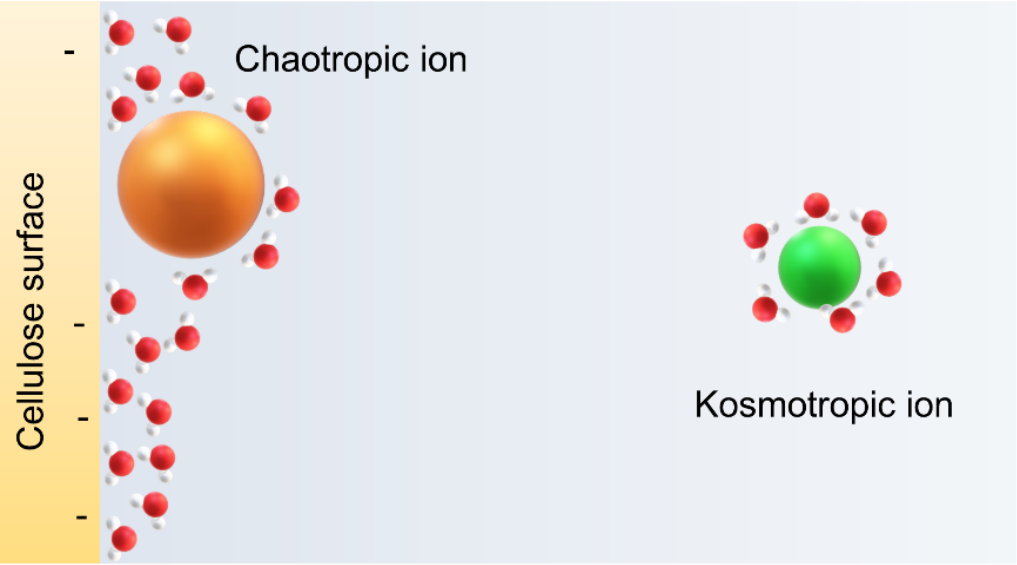

Figure 8.5. Hydration dictated the distribution of anions in the cellulose-water interface.

The charges in cellulose originated due to the presence of hemicellulose, the distribution of these charges will be non-uniform and we could consider it a patchy surface. The anions might interact with the hydrophobic domains of the cellulose exposed to the water. However, how could the accumulation of chaotropic anions alter CMC's adsorption on cellulose surface? To answer this question, the driving force of the adsorption of polymers should be considered.

We have seen in chapter 3 that the entropy gain drives the adsorption of CMC on the cellulose surface due to the release of unfavourably arranged water molecules on the surface. The distribution of ions at a charged interface plays a crucial role in determining the effect of charge on the water organization[81]. The vicinity of chaotropic nitrate ion at the interface could be causing a more unfavourable organization of water molecules at the interface, which results in larger entropy gain once released from the surface and thus higher adsorption of CMC.

This anion-cation pairing may have an effect on how an ion interacts with interfaces[96,150,151]. According to LWMA, ions form stronger contact ion pairs if

their hydration behaviour is comparable, allowing their hydration shells to be shared. Sulfate ions with a B-coefficient of 0.208 exhibit similar hydration behaviour to magnesium ions with a B-coefficient of 0.385, and they frequently form stable contact ion pairs. Magnesium ions may be drawn away from the interface by sulfate ions, limiting magnesium ion availability at the interface. In comparison, the hydration enthalpy of nitrate (B-coefficient = -0.046) and magnesium (B-coefficient = 0.385) ions is significantly different, showing that these ions may behave as well-separated ions with 'independent' mobility. According to Xu et al.[151] the ion pairing of interfacial nitrate ions and magnesium ions is negligible, and nitrate anions in the air-aqueous interfacial area are essentially unaffected by magnesium ion Coulombic effects. This 'independent mobility' of magnesium and nitrate ions contributes to their availability at the interface, affecting CMC's adsorption on cellulose surfaces.

Chapter 9

Concluding remarks

This thesis sought to study carboxymethyl cellulose's adsorption on cellulose, prompted by the necessity to integrate it into the existing pulping infrastructure. Adsorption studies with deuterated water and water as the solvent for CMC demonstrated that the release of water molecules from the cellulose and CMC surfaces plays a substantial role in driving the adsorption. Temperature-dependent adsorption experiments on cellulose model films further supported an entropy-driven mechanism. ITC studies were conducted to determine the thermodynamic profile of CMC adsorption on the surface of cellulose. It was discovered that the binding of CMC to the cellulose surface did not result in a substantial heat change. The data collected from ITC were insufficient for conducting analysis to extract thermodynamic parameters. However, the very faint heat signals in the ITC thermogram show that the CMC adsorption on the cellulose surface is entropy-driven. Because entropy is the primary driving force, the adsorption step should be combined with a high-temperature bleaching stage.

One of the significant challenges in integrating the CMC adsorption step with the pulping process is identifying an industrially viable electrolyte to enhance adsorption. Ca^{2+} ions are known to improve the adsorption; however, they cannot be used in an industrial setting due to the scaling problems. Therefore, magnesium ions were identified as a suitable alternative. However, adsorption studies conducted on model cellulose surface and commercially available cellulose-rich fibers revealed that CMC adsorption is prone to cation specific effects, and Mg^{2+} ions were less efficient in enhancing the adsorption than Ca^{2+}. The increased adsorption of CMC in presence of Ca^{2+} ions is ascribed to dispersion interactions caused due to the larger polarizability of the Ca^{2+} ions.

It was known that the divalent ions have a significant effect on CMC adsorption, and Ca^{2+} was thought to act as a bridge between the CMC chain and the negatively charged cellulose surface to make adsorption possible. However, previous studies on the adsorption of CMC on cellulose and negatively charged polyelectrolytes, in general, have missed the changes in the polymer solution's characteristics when multivalent ions such as Ca^{2+} are present. Therefore, the effect of divalent ions on the adsorption of CMC onto cellulose was investigated in this thesis from the perspective that the adsorption process is multifaceted and can be influenced by the cellulose surface and solution properties. Dynamic light scattering tests on CMC solutions containing different ionic strengths of

$CaCl_2$ found that the addition of $CaCl_2$ enhanced the hydrodynamic size of CMC. Additionally, a correlation was observed between the hydrodynamic diameter of CMCs at various ionic strengths of $CaCl_2$ and the amount of CMC adsorbed at those ionic strengths. This reveals that the adsorption of CMCs at high $CaCl_2$ concentrations is mainly regulated by structural changes in the CMC solution, which effectively diminish polymer-solvent interactions and hence contribute to the adsorption driving force.

As mentioned before, magnesium ions were found to be a good alternative for Ca^{2+} ions. Thoughts to improve the efficiency of the Mg^{2+} system in enhancing adsorption of CMC has led to the study of co-anion specific effects in adsorption of CMC. Generally, it is believed that co-anions are excluded from the interface and do not influence interfacial processes such as adsorption. The results in this thesis suggest that CMC adsorption can be tuned by changing the co-anions. The degree of hydration of anions influences how these anions are distributed at the interface, influencing the water organisation at the interface and thus CMC adsorption. The co-anion specificity observed for CMC adsorption in the presence of magnesium salts enables us to tailor CMC adsorption by selecting the appropriate combination of Mg^{2+} ion and co-anions, and therefore obtain high adsorption without causing scaling difficulties.

Chapter 10

Future Outlook

The model adsorption experiments in this thesis suggested that magnesium nitrates can be used to improve the CMC adsorption without causing scaling issues. However, this should be validated by performing CMC adsorptions on the cellulose-rich fiber during the bleaching stage. Currently, magnesium sulfates are used as a source of magnesium ions in the industry. Changing this to magnesium nitrate could have an adverse effect on the properties of paper, especially optical properties. Therefore, the effect of magnesium nitrate on the final properties of the modified pulp should be studied in detail

As usual, gaining increased understanding often leads to even more questions and new ideas to move forward. For example, one of the major questions that arose during the thesis was how hemicellulose located at the surface influence the adsorption of CMC? Therefore, it would be interesting to perform adsorption studied in fibers with different hemicellulose content

In chapter 8, we saw that the adsorption of CMC on cellulose is anion specific. Since the charges in the fibers used in the study mainly originated from hemicellulose, the distribution of these charges on the cellulose surface might be random. It could be interesting to look into the anion specificity in adsorption of CMC on cellulose surfaces with different charge density and distribution, for example, a TEMPO-oxidized cellulose nanofiber films where the charges are relatively evenly distributed compared to unmodified CNF, and a regenerated cellulose surface with no significant anionic groups (that is also uniform in terms of structure) compared to cellulose nanofiber films.

Anion specificity observed in CMC adsorption is suggested to be due to the difference in the distribution of ions at the interface and the ordering of water molecules at the interface. The orientation of water molecules at the interface and ions specificity should be investigated further using high-resolution techniques such as Vibrational Sum Frequency Spectroscopy (VSFS). Furthermore, molecular dynamic simulations could be used to get more detailed information.

References

(1) Bellis, M. The Invention of the Wheel. https://www.thoughtco.com/the-invention-of-the-wheel-1992669. Accessed on 22/01/2022

(2) Berna, F.; Goldberg, P.; Horwitz, L. K.; Brink, J.; Holt, S.; Bamford, M.; Chazan, M. Microstratigraphic Evidence of in Situ Fire in the Acheulean Strata of Wonderwerk Cave, Northern Cape Province, South Africa. *Proc. Natl. Acad. Sci. U. S. A.* **2012**, *109* (20), p 1215. https://doi.org/10.1073/pnas.1117620109.

(3) Kumar, D. U.; Sreekumar, G. V; Athvankar, U.A. Traditional Writing System in Southern India — Palm Leaf Manuscripts . *Des. Thoughts* **2009**, p2. http://www.idc.iitb.ac.in/resources/dt-july-2009/Palm.pdf

(4) Alexander Stille. The World's Oldest Papyrus and What It Can Tell Us About the Great Pyramids. *Smithsonian Magazine*. Oct **2015**. https://www.smithsonianmag.com. Accessed on 22/01/2022

(5) Cantavalle, S. The History of Paper: From its Origins to The Present Day https://www.pixartprinting.co.uk/blog/history-paper/. Accessed on 22/02/2022

(6) *Specialty Paper Market By Product Type (Décor, Thermal, Carbonless, Kraft, Other Types), End Use Application (Printing and Writing, Packaging, Building and Construction, Industrial, Other Commercial End Use) & Region – Forecast 2021 – 2031*; **2021**. https://www.futuremarketinsights.com/reports/specialty-paper-market

(7) Johansson, K.; Wilhelmsson, L.; Holmberg, H.; Lindström, T.; Lagerström, J.; Persson, T. *Swedish Forest-Based Sector Research Agenda 4.0, For GrowthIn The Worls's Bioeconomy*; **2018**.

(8) Hasani, M. Chemical Modification of Cellulose ; New Possibilities of Some Classical Routes, Disp Chalmers University of Technology, **2010**. https://doi.org/10.1201/9781315139142.

(9) Arumughan, V.; Nypelö, T.; Hasani, M.; Larsson, A. Fundamental Aspects of the Non-Covalent Modification of Cellulose via Polymer Adsorption. *Adv. Colloid Interface Sci.* **2021**, *298*, p 102529. https://doi.org/10.1016/j.cis.2021.102529.

(10) Wågberg, L.; Odberg, L. Polymer Adsorption on Cellulosic Fibers. *Nord. Pulp Pap. Res. J.* **2007**, *4* (2), p135. https://doi.org/10.3183/npprj-1989-04-02-p135-140.

(11) Ekevåg, P.; Lindström, T.; Gellerstedt, G.; Lindström, M. E. Addition of Carboxymethyl cellulose to the Kraft Cook. *Nord. Pulp Pap. Res. J.* **2004,** *19*(2), p200. https://doi.org/10.3183/npprj-2004-19-02-p200-207.

(12) Laine, J.; Lindström, T.; Glad Nordmark, G.; Risinger, G. Studies on Topochemical Modification of Cellulosic Fibres. Part 2. *Nord. Pulp Pap. Res.J.* **2002**, *17* (1), p50. https://doi.org/10.3183/npprj-2002-17-01-p050-056.

(13) Kontturi, E.; Mitikka-Eklund, M.; Vuorinen, T. Strength Enhancement of a Fiber Network by Carboxymethyl Cellulose during Oxygen Delignification of Kraft Pulp. *BioResources* **2008,** *3*(1) p34**.** https://doi.org/10.15376/biores.3.1.34-45.

(14) Butchosa, N.; Zhou, Q. Water Redispersible Cellulose Nanofibrils Adsorbed with Carboxymethyl Cellulose. *Cellulose* **2014**, *21* (6), p4349. https://doi.org/10.1007/s10570-014-0452-7.

(15) Azrak, S. M. E. A.; Gohl, J. A.; Moon, R. J.; Schueneman, G. T.; Davis, C. S.; Youngblood, J. P. Controlled Dispersion and Setting of Cellulose Nanofibril - Carboxymethyl Cellulose Pastes. *Cellulose* **2021**, *28* (14), p9149. https://doi.org/10.1007/s10570-021-04081-5.

(16) Agarwal, D.; MacNaughtan, W.; Foster, T. J. Interactions between Microfibrillar Cellulose and Carboxymethyl Cellulose in an Aqueous Suspension. *Carbohydr. Polym.* **2018**, *185*, p112. https://doi.org/10.1016/j.carbpol.2017.12.086.

(17) Ek, M.; Gellerstedt, G.; Henriksson, G. *Wood Chemistry and Biotechnology*, Volume 1.; Walter de Gruyter., **2009**.

(18) Kerr, AJ.; Goring, D. The Ultrastructure Arrangement of the Wood Cell Wall. *Cell Chem Tech* **1975**, *9*, p563.

(19) Burgert, I. Exploring the Micromechanical Design of Plant Cell Walls. *Am. J. Bot.* **2006**, *93* (10), p1391. https://doi.org/10.3732/ajb.93.10.1391.

(20) Cosgrove, D. J. Growth of the Plant Cell Wall. *Nat. Rev. Mol. Cell Biol.* **2005**, *6* (11), p850. https://doi.org/10.1038/nrm1746.

(21) Nishimura, H.; Kamiya, A.; Nagata, T.; Katahira, M.; Watanabe, T. Direct Evidence for α Ether Linkage between Lignin and Carbohydrates in Wood Cell Walls. *Sci. Rep.* **2018**, *8* (1), p1. https://doi.org/10.1038/s41598-018-24328-9.

(22) Brännvall, E. Overview of Pulp and Paper Processes. In *The Ljungberg Textbook - Wood Chemistry*; **2008**.

(23) Chakar, F. S.; Ragauskas, A. J. Review of Current and Future Softwood Kraft Lignin Process Chemistry. *Ind. Crops Prod.* **2004**, *20* (2), p131. https://doi.org/10.1016/j.indcrop.2004.04.016.

(24) Aurell, R. Hartler, N. Kraft Pulping of Pine. II. Influence of the Charge of Alkalio on the Yield, Carbohydrate Composition, and Properties of the Pulp. *Sven. Papperstidn* **1965**, *68*(4), p97.

(25) Henriksson, G. The Chemistry of Bleaching. In *The Ljungberg Textbook - Cellulose Technology*; KTH: Stockholm, **2008**.

(26) Germgård, U. Bleaching of Pulp. In *The Ljungberg Textbook - Cellulose Technology*; KTH: Stockholm, **2008**.

(27) Stone, J.E.; Scallan, A. M. The Effect of Component Removal upon the Porous Structure of the Cell Wall of Wood. Part III. A Comparison between the Sulphite and Kraft Process. *Pulp Pap. Mag. Canada* **1968**, *69*, p288.

(28) Fahlén, J.; Salmén, L. Ultrastructural Changes in a Holocellulose Pulp Revealed by Enzymes, Thermoporosimetry and Atomic Force Microscopy. *Holzforschung* **2005**, *59* (6), p589. https://doi.org/10.1515/HF.2005.096.

(29) Fahlén, J.; Salmén, L. Pore and Matrix Distribution in the Fiber Wall Revealed by Atomic Force Microscopy and Image Analysis. *Biomacromolecules* **2005**, *6* (1), p433. https://doi.org/10.1021/bm040068x.

(30) Duchesne, I.; Daniel, G. The Ultrastructure of Wood Fibre Surfaces as Shown by a Variety of Microscopical Methods - A Review. *Nord. Pulp Pap. Res. J.* **1999**, *14* (2), p129. https://doi.org/10.3183/npprj-1999-14-02-p129-139.

(31) Andreasson, B.; Forsström, J.; Wågberg, L. The Porous Structure of Pulp Fibres with Different Yields and Its Influence on Paper Strength. *Cellulose* **2003**, *10* (2), p111. https://doi.org/10.1023/A:1024055406619.

(32) Wågberg, Lars. "Polyelectrolyte adsorption onto cellulose fibres – A review" *Nord. Pulp Pap. Res. J.* **2000,** *15*, p. 586. https://doi.org/10.3183/npprj-2000-15-05-p586-597

(33) Jedvert, K.; Heinze, T. Cellulose Modification and Shaping - A Review. *J. Polym. Eng.* **2017**, *37* (9), p845. https://doi.org/10.1515/polyeng-2016-0272.

(34) Tang, J.; Sisler, J.; Grishkewich, N.; Tam, K. C. Functionalization of Cellulose Nanocrystals for Advanced Applications. *J. Colloid Interface Sci.* **2017,** *494*, p397. https://doi.org/10.1016/j.jcis.2017.01.077.

(35) Voisin, H.; Bergström, L.; Liu, P.; Mathew, A. P. Nanocellulose-Based Materials for Water Purification. **2017,** *7*(3), p57. https://doi.org/10.3390/nano7030057.

(36) Tsuji, W.; Nakao, T.; Ohigashi, K.; Maegawa, K.; Kobayashi, N.; Shukri, S.; Kasai, S.; Miyanaga, K. Chemical Modification of Cotton Fiber by Alkali-swelling and Substitution Reactions—Acetylation, Cyanoethylation, Benzoylation, and Oleoylation. *J. Appl. Polym. Sci.* **1986**, *32* (5), p5175. https://doi.org/10.1002/app.1986.070320533.

(37) Swensson, B.; Larsson, A.; Hasani, M. Dissolution of Cellulose Using a Combination of Hydroxide Bases in Aqueous Solution. *Cellulose* **2020**, *27* (1), p101. https://doi.org/10.1007/s10570-019-02780-8.

(38) Gunnarsson, M.; Theliander, H.; Hasani, M. Chemisorption of Air CO2 on Cellulose: An Overlooked Feature of the Cellulose/NaOH(Aq) Dissolution System. *Cellulose* **2017,** *24*, p2427. https://doi.org/10.1007/s10570-017-1288-8.

(39) Barzyk, D.; Page,D.; and Ragsuskas, A. Acidic Group Topochemistry and Fibre-to-Fibre Specific Bond Strength. *J. Pulp Pap. Sci.* **1996**, *26* (4), p551.

(40) Barzyk, D. H. P. and A. R. Carboxylic Acid Groups and Fi Bre Bonding. In The Fundametals of Papermaking Materials. Trans. of the XIth Fund. Res. Symp. Cambridge, **1997**, (C.F. Baker, ed.), p893.

(41) Laine, J.; Lindström, T.; Studies on Topochemical Modification of Cellulosic Fibres. Part 1. Chemical Conditions for the Attachment of Carboxymethyl Cellulose onto Fibres. *Nordic Pulp and Paper Research Journal*. **2000**, *15*(5), p520. https://doi.org/10.3183/NPPRJ-2000-15-05-p520-526.

(42) Danielsson, S. *Xylan Reactions in Kraft Cooking Process and Product Considerations*; Disp KTH, **2007**.

(43) Danielsson, Sverker.; Lindström, Mi. Influence of Birch Xylan Adsorption during Kraft Cooking on Softwood Pulp Strength. *Nord. Pulp Pap. Res. J.* **2018**, *20* (4), p436. https://doi.org/https://doi.org/10.3183/npprj-2005-20-04-p436-441.

(44) Orelma, H.; Filpponen, I.; Johansson, L. S.; Laine, J.; Rojas, O. J. Modification of Cellulose Films by Adsorption of Cmc and Chitosan for Controlled Attachment of Biomolecules. *Biomacromolecules* **2011**, *12*(12), p4311 . https://doi.org/10.1021/bm201236a.

(45) Orelma, H.; Teerinen, T.; Johansson, L. S.; Holappa, S.; Laine, J. CMC-Modified Cellulose Biointerface for Antibody Conjugation. *Biomacromolecules* **2012,** *13*(4), p1051. https://doi.org/10.1021/bm201771m.

(46) Sjostrom, E. The Origin of Charge on Cellulosic Fibers. *Nord. Pulp Pap. Res. J.* **2007**, *4* (2), p90. https://doi.org/10.3183/npprj-1989-04-02-p090-093.

(47) Martien, Cohen Stuart. Terenc, Cosgrove. Vincent, B. Experimental Aspects of Polymer Adsorption at Solid/Solution Interfaces. **1986**, *24*, p143. https://doi.org/10.1016/0001-8686(85)80030-0.

(48) Kontturi, E.; Tammelin, T.; Österberg, M. Cellulose - Model Films and the Fundamental Approach. *Chemical Society Reviews*. 2006, *35*, p1287. https://doi.org/10.1039/b601872f.

(49) Kontturi, E.; Spirk, S. Ultrathin Films of Cellulose: A Materials Perspective. *Frontiers in Chemistry*.**2019,** *7*, p488. https://doi.org/10.3389/fchem.2019.00488.

(50) Zhang, L.; Ruan, D.; Zhou, J. Structure and Properties of Regenerated Cellulose Films Prepared from Cotton Linters in NaOH/Urea Aqueous Solution. *Ind. Eng. Chem. Res.* **2001**, *40* (25). https://doi.org/10.1021/ie0010417.

(51) Neuman, R. D.; Berg, J. M.; Claesson, P. M. Direct Measurement of Surface Forces in Papermaking and Paper Coating Systems. *Nord. Pulp Pap. Res. J.* **2007**, *8* (1). https://doi.org/10.3183/npprj-1993-08-01-p096-104.

(52) Kargl, R.; Mohan, T.; Bračč, M.; Kulterer, M.; Doliška, A.; Stana-Kleinschek, K.; Ribitsch, V. Adsorption of Carboxymethyl Cellulose on Polymer Surfaces: Evidence of a Specific Interaction with Cellulose. *Langmuir* **2012**, *28*(31), p11440. https://doi.org/10.1021/la302110a.

(53) Liu, Z.; Choi, H.; Gatenholm, P.; Esker, A. R. Quartz Crystal Microbalance with Dissipation Monitoring and Surface Plasmon Resonance Studies of Carboxymethyl Cellulose Adsorption onto Regenerated Cellulose Surfaces. *Langmuir* **2011**, *27*(14), p8718.

(54) Mohan, T.; Kargl, R.; Doliška, A.; Vesel, A.; Köstler, S.; Ribitsch, V.; Stana-Kleinschek, K. Wettability and Surface Composition of Partly and Fully Regenerated Cellulose Thin Films from Trimethylsilyl Cellulose. *J. Colloid Interface Sci.* **2011**, *358* (2), p604. https://doi.org/10.1016/j.jcis.2011.03.022.

(55) Mohan, T.; Spirk, S.; Kargl, R.; Doliška, A.; Vesel, A.; Salzmann, I.; Resel, R.; Ribitsch, V.; Stana-Kleinschek, K. Exploring the Rearrangement of Amorphous Cellulose Model Thin Films upon Heat Treatment. *Soft Matter* **2012**, *8* (38), p9807. https://doi.org/10.1039/c2sm25911g.

(56) Wolfberger, A.; Kargl, R.; Griesser, T.; Spirk, S. Photoregeneration of Trimethylsilyl Cellulose as a Tool for Microstructuring Ultrathin Cellulose Supports. *Molecules* **2014**, *19* (10), p16266. https://doi.org/10.3390/molecules191016266.

(57) Jones, A. O. F.; Resel, R.; Schrode, B.; Machado-Charry, E.; Röthel, C.; Kunert, B.; Salzmann, I.; Kontturi, E.; Reishofer, D.; Spirk, S. Structural Order in Cellulose Thin Films Prepared from a Trimethylsilyl Precursor. *Biomacromolecules* **2020**, *21* (2), p653. https://doi.org/10.1021/acs.biomac.9b01377.

(58) Edgar, C. D.; Gray, D. G. Smooth Model Cellulose I Surfaces from Nanocrystal Suspensions. *Cellulose* **2003**, *10* (4). https://doi.org/10.1023/A:1027333928715.

(59) Ahola, S.; Salmi, J.; Johansson, L. S.; Laine, J.; Österberg, M. Model Films from Native Cellulose Nanofibrils. Preparation, Swelling, and Surface Interactions. *Biomacromolecules* **2008**, *9*(4), p1273. https://doi.org/10.1021/bm701317k.

(60) Nypelö, T.; Pynnönen, H.; Österberg, M.; Paltakari, J.; Laine, J. Interactions between Inorganic Nanoparticles and Cellulose Nanofibrils. *Cellulose* **2012**, *19* (3), p779. https://doi.org/10.1007/s10570-012-9656-x.

(61) Niegelhell, K.; Chemelli, A.; Hobisch, J.; Griesser, T.; Reiter, H.; Hirn, U.; Spirk, S. Interaction of Industrially Relevant Cationic Starches with Cellulose. *Carbohydr. Polym.* **2018**, *179*, p290. https://doi.org/10.1016/j.carbpol.2017.10.003.

(62) Villares, A.; Moreau, C.; Dammak, A.; Capron, I.; Cathala, B. Kinetic Aspects of the Adsorption of Xyloglucan onto Cellulose Nanocrystals. *Soft Matter* **2015**, *11*, p6472. https://doi.org/10.1039/c5sm01413a.

(63) Winter, L.; Wågberg, L.; Ödberg, L.; Lindström, T. Polyelectrolytes Adsorbed on the Surface of Cellulosic Materials. *J. Colloid Interface Sci.* **1986**, *111* (2), p537. https://doi.org/10.1016/0021-9797(86)90057-3.

(64) Lindström, T . Wågberg, L. Effects of PH and Electrolyte Concentration on the Adsorption of Cationic Polyacylamides on Cellulose. *Tappi.* **1983**, *66* (6), p83.

(65) Fu, J.; Schlenoff, J. B. Driving Forces for Oppositely Charged Polyion Association in Aqueous Solutions: Enthalpic, Entropic, but Not Electrostatic. *J. Am. Chem. Soc.* **2016**, *138* (3), p980. https://doi.org/10.1021/jacs.5b11878.

(66) Reid, M. S.; Villalobos, M.; Cranston, E. D. The Role of Hydrogen Bonding in Non-Ionic Polymer Adsorption to Cellulose Nanocrystals and Silica Colloids. *Current Opinion in Colloid and Interface Science*. **2017**, *29*, p76**.** https://doi.org/10.1016/j.cocis.2017.03.005.

(67) G. J. Fleer, M. A. Cohen Stuart, J. M. H. M. Scheutjens, T. Cosgrove and B. Vincent. Polymers at Interfaces,Springer Science and Bussiness media **1993.**

(68) van de Steeg, H. G. M.; Stuart, M. A. C.; de keizer, A.; Bijsterbosch, B. H. Polyelectrolyte Adsorption: A Subtle Balance of Forces. *Langmuir* **1992**, *8* (10), p2538. https://doi.org/10.1021/la00046a030.

(69) Wågberg, L.; Bjorklund, M. Adsorption of Cationic Potato Starch on Cellulosic Fibres. *Nord. Pulp Pap. Res. J.***1993**, *8*(4), p399. https://doi.org/10.3183/npprj-1993-08-04-p399-404.

(70) Wådgberg, L.; Odberg, L.; Glad-Nordmark, G. Charge Determination of Porous Substrates by Polyelectrolyte Adsorption. *Nord. Pulp Pap. Res. J.* **1989,** *4*(2), p71. https://doi.org/10.3183/npprj-1989-04-02-p071-076.

(71) Wågberg, L., Ödberg, L. and Glad-Nordmark, G. Charge Determination of Porous Substrates by Polyelectrolyte Adsorption. Part 1. Carboxymethylated, Bleached Cellulosic Fibres. *Nord. Pulp Pap. Res. J* **1989**, *4* (2), p71.

(72) Heinze, T.; Liebert, T.; Klüfers, P.; Meister, F. Carboxymethylation of Cellulose in Unconventional Media. *Cellulose* **1999,** *6,* p153. https://doi.org/10.1023/A:1009271427760.

(73) Fechter, C.; Heinze, T. Influence of Wood Pulp Quality on the Structure of Carboxymethyl Cellulose. *J. Appl. Polym. Sci.* **2019**, *136*(34), p47862. https://doi.org/10.1002/app.47862.

(74) Lopez, C. G.; Rogers, S. E.; Colby, R. H.; Graham, P. Structure of Sodium Carboxymethyl Cellulose Aqueous Solutions : A SANS and Rheology Study. Journal of Polymer Science Part B. **2015** , *53*(7), p492 https://doi.org/10.1002/polb.23657.

(75) Mierczynska-Vasilev, A.; Beattie, D. A. Adsorption of Tailored Carboxymethyl Cellulose Polymers on Talc and Chalcopyrite: Correlation between Coverage, Wettability, and Flotation. *Miner. Eng.* **2010**, *23* (11–13), p985. https://doi.org/10.1016/j.mineng.2010.03.025.

(76) Bicak, O.; Ekmekci, Z.; Bradshaw, D. J.; Harris, P. J. Adsorption of Guar Gum and CMC on Pyrite. *Miner. Eng.* **2007,** *20*(10), p996. https://doi.org/10.1016/j.mineng.2007.03.002.

(77) Fras Zemljič, L.; Stenius, P.; Laine, J.; Stana-Kleinschek, K. Topochemical Modification of Cotton Fibres with Carboxymethyl Cellulose. *Cellulose* **2008**, *15*, p315. https://doi.org/10.1007/s10570-007-9175-3.

(78) Turesson, M.; Labbez, C.; Nonat, A. Calcium Mediated Polyelectrolyte Adsorption on Like-Charged Surfaces. *Langmuir* **2011**, *27*(22) p13572. https://doi.org/10.1021/la2030846.

(79) Tiraferri, A.; Maroni, P.; Borkovec, M. Adsorption of Polyelectrolytes to Like-Charged Substrates Induced by Multivalent Counterions as Exemplified by Poly(Styrene Sulfonate) and Silica. *Phys. Chem. Chem. Phys.* **2015**, *17*, p10348. https://doi.org/10.1039/c5cp00910c.

(80) Bonthuis, D. J.; Gekle, S.; Netz, R. R. Dielectric Profile of Interfacial Water and Its Effect on Double-Layer Capacitance. *Phys. Rev. Lett.* **2011**, *107* (16), p1. https://doi.org/10.1103/PhysRevLett.107.166102.

(81) Gonella, G.; Backus, E. H. G.; Nagata, Y.; Bonthuis, D. J.; Loche, P.; Schlaich, A.; Netz, R. R.; Kühnle, A.; McCrum, I. T.; Koper, M. T. M.; Wolf, M.; Winter, B.; Meijer, G.; Campen, R. K.; Bonn, M. Water at Charged Interfaces. *Nat. Rev. Chem.* **2021**, *5* (7), p466. https://doi.org/10.1038/s41570-021-00293-2.

(82) Helmholtz, H. Ueber Einige Gesetze Der Vertheilung Elektrischer Ströme in Körperlichen Leitern, Mit Anwendung Auf Die Thierisch-Elektrischen Versuche (Schluss.). *Ann. Phys.* **1853**, *165* (7), p353. https://doi.org/https://doi.org/10.1002/andp.18531650702.

(83) Helmholtz, H. Studien Über Electrische Grenzschichten. *Ann. Phys.* **1879**, *243* (7), p337. https://doi.org/https://doi.org/10.1002/andp.18792430702.

(84) Grahame, D. The Electrical Double Layer and the Theory of Electrocapillarity. *Chemical* **1947**, *43* (3), p441.

(85) Gouy, M.; Sur la constitution de la charge électrique à la surface d'un électrolyte . J. Phys. Theor. Appl., **1910**, *9*(1), p457

(86) Chapman, D. L. A Contribution to the Theory of Electrocapillarity. **1913,** 148(25), p*5982*. https://doi.org/10.1080/14786440408634187.

(87) Brad, A.J. ; Faulkner, L. . *Electrochemical Methods; Fundamentals and Applications*, 2nd ed.; Wiley, **2000**.

(88) Stern, O. Zur Theorie Der Elektrolytischen Doppelschicht. *Zeitschrift für Elektrochemie und Angew. Phys. Chemie* **1924**, *30* (21–22), p508.

(89) Laage, D.; Elsaesser, T.; Hynes, J. T.; Normale, E. Water Dynamics in the Hydration Shells of Biomolecules. **2017,** *117*(16), p10694. https://doi.org/10.1021/acs.chemrev.6b00765.

(90) Debe, M. K. Electrocatalyst Approaches and Challenges for Automotive Fuel Cells. *Nature* **2012**, *486* (7401), p43. https://doi.org/10.1038/nature11115.

(91) Shpigel, N.; Chakraborty, A.; Malchik, F.; Bergman, G.; Nimkar, A.; Gavriel, B.; Turgeman, M.; Hong, C. N.; Lukatskaya, M. R.; Levi, M. D.; Gogotsi, Y.; Major, D. T.; Aurbach, D. Can Anions Be Inserted into MXene? **2021**, *143*(32) p12552. https://doi.org/10.1021/jacs.1c03840.

(92) Shpigel, Netanel; ; Levi, Mikhael D. ; Sigalov, Sergey; Mathis, Tyler S. ; Gogosti, Y. Direct Assessment of Nanocon Fined Water in 2D Ti 3 C 2 Electrode Interspaces by a Surface Acoustic Technique. *J. Am. Chem. Soc.* **2018**, *140*, p8910. https://doi.org/10.1021/jacs.8b04862.

(93) Marcus, Y. Effect of Ions on the Structure of Water. *Pure Appl. Chem.* **2010**, *82* (10), p1889. https://doi.org/10.1351/PAC-CON-09-07-02.

(94) Parsons, D. F.; Boström, M.; Nostro, P. Lo; Ninham, B. W. Hofmeister Effects: Interplay of Hydration, Nonelectrostatic Potentials, and Ion Size. *Phys. Chem. Chem. Phys.* **2011**, *13* (27), p12352. https://doi.org/10.1039/c1cp20538b.

(95) Boström, M.; Williams, D. R. M.; Ninham, B. W. Specific Ion Effects: Why DLVO Theory Fails for Biology and Colloid Systems. *Phys. Rev. Lett.* **2001,** *87*, p168103. https://doi.org/10.1103/PhysRevLett.87.168103.

(96) Salis, A.; Ninham, B. W. Models and Mechanisms of Hofmeister Effects in Electrolyte Solutions, and Colloid and Protein Systems Revisited. *Chemical Society Reviews*. **2014**, *43*, p7358. https://doi.org/10.1039/c4cs00144c.

(97) Ninham, B. W.; Yaminsky, V. Ion Binding and Ion Specificity: The Hofmeister Effect and Onsager and Lifshitz Theories. *Langmuir* **1997**, *13* (7), p2097. https://doi.org/10.1021/la960974y.

(98) Hofmeister, F. Zur Lehre von Der Wirkung Der Salze - Dritte Mittheilung. *Arch. für Exp. Pathol. und Pharmakologie* **1888**, *25* (1), p1. https://doi.org/10.1007/BF01838161.

(99) Kunz, W.; Henle, J.; Ninham, B. W. "Zur Lehre von Der Wirkung Der Salze" (about the Science of the Effect of Salts): Franz Hofmeister's Historical Papers. *Curr. Opin. Colloid Interface Sci.* **2004**, *9* (1–2), p19. https://doi.org/10.1016/j.cocis.2004.05.005.

(100) Jone, Grinnel; Dole, M. The Viscosity of Aqueous Solutions of Strong Electrolytes with Special Reference to Barium Chloride. *J. Am. Chem. Soc.* **1929**, *51*, p2950. https://doi.org/10.1021/ja01385a012.

(101) Schwierz, N.; Horinek, D.; Netz, R. R. Anionic and Cationic Hofmeister Effects on Hydrophobic and Hydrophilic Surfaces. *Langmuir* **2013**, *29* (8), p2602. https://doi.org/10.1021/la303924e.

(102) Salis, A.; Ninham, B. W. Models and Mechanisms of Hofmeister Effects in Electrolyte Solutions, and Colloid and Protein Systems Revisited. *Chem. Soc. Rev.* **2014**, *43* (21), p7358. https://doi.org/10.1039/c4cs00144c.

(103) Ries-Kautt, M. M.; Ducruix, A. F. Relative Effectiveness of Various Ions on the Solubility and Crystal Growth of Lysozyme. *J. Biol. Chem.* **1989**, *264* (2), p745. https://doi.org/10.1016/s0021-9258(19)85005-6.

(104) Zhang, Y.; Cremer, P. S. The Inverse and Direct Hofmeister Series for Lysozyme. *Proc. Natl. Acad. Sci. U. S. A.* **2009**, *106* (36), p15249. https://doi.org/10.1073/pnas.0907616106.

(105) Omta, A. W.; Kropman, M. F.; Woutersen, S.; Bakker, H. J. Negligible Effect of Ions on the Hydrogen-Bond Structure in Liquid Water. *Science.* **2003**, *301*(5631), p347. https://www.science.org/doi/10.1126/science.1084801.

(106) Collins, K. D. Charge Density-Dependent Strength of Hydration and Biological Structure. *Biophys. J.* **1997**, *72* (1), p65. https://doi.org/10.1016/S0006-3495(97)78647-8.

(107) Marcus, Y.; Hefter, G. Ion Pairing. *Chem. Rev.* **2006**, *106* (11), p4585. https://doi.org/10.1021/cr040087x.

(108) Vlachy, N.; Jagoda-Cwiklik, B.; Vácha, R.; Touraud, D.; Jungwirth, P.; Kunz, W. Hofmeister Series and Specific Interactions of Charged Headgroups with Aqueous Ions. *Adv. Colloid Interface Sci.* **2009**, *146* (1–2), p42. https://doi.org/10.1016/j.cis.2008.09.010.

(109) Lifshitz, E. M. The Theory of Molecular Attractive Forces between Solids. *In Perspectives in Theoretical Physics* **1992**,p 329. https://doi.org/10.1016/b978-0-08-036364-6.50031-4.

(110) Mittal, N.; Benselfelt, T.; Ansari, F.; Gordeyeva, K.; Roth, S. V.; Wågberg, L.; Söderberg, L. D. Ion-Specific Assembly of Strong, Tough, and Stiff Biofibers. *Angewandte Chemie - International Edition*. **2019,** *131*(51), p18735. https://doi.org/10.1002/anie.201910603.

(111) Benselfelt, T.; Nordenström, M.; Hamedi, M. M.; Wågberg, L. Ion-Induced Assemblies of Highly Anisotropic Nanoparticles Are Governed by Ion-Ion Correlation and Specific Ion Effects. *Nanoscale* **2019**, *11*, p3514. https://doi.org/10.1039/c8nr10175b.

(112) Zhang, Y.; Yang, F.; Hu, F.; Song, J.; Wu, S.; Jin, Y. Binding Preference of Family 1 Carbohydrate Binding Module on Nanocrystalline Cellulose and Nanofibrillar Cellulose Films Assessed by Quartz Crystal Microbalance. *Cellulose* **2018**, *25* (6), p3327. https://doi.org/10.1007/s10570-018-1803-6.

(113) Zhang, Y.; Wang, X.; Wang, P.; Song, J.; Jin, Y.; Rojas, O. J. Interactions between Type A Carbohydrate Binding Modules and Cellulose Studied with a Quartz Crystal Microbalance with Dissipation Monitoring. *Cellulose* **2020**, *27* (7), p3661. https://doi.org/10.1007/s10570-020-03070-4.

(114) Liu, T.; Zhang, Y.; Lu, X.; Wang, P.; Zhang, X.; Tian, J.; Wang, Q.; Song, J.; Jin, Y.; Xiao, H. Binding Affinity of Family 4 Carbohydrate Binding Module on Cellulose Films of Nanocrystals and Nanofibrils. *Carbohydr. Polym.* **2021**, *251* p116725. https://doi.org/10.1016/j.carbpol.2020.116725.

(115) Latour, R. A. The Langmuir Isotherm: A Commonly Applied but Misleading Approach for the Analysis of Protein Adsorption Behaviour. *J. Biomed. Mater. Res. - Part A* **2015**, *103* (3), p949. https://doi.org/10.1002/jbm.a.35235.

(116) Kishani, S.; Benselfelt, T.; Wågberg, L.; Wohlert, J. Entropy Drives the Adsorption of Xyloglucan to Cellulose Surfaces – A Molecular Dynamics Study. *J. Colloid Interface Sci.* **2021**, *588,* p485. https://doi.org/10.1016/j.jcis.2020.12.113.

(117) Benselfelt, T.; Cranston, E. D.; Ondaral, S.; Johansson, E.; Brumer, H.; Rutland, M. W.; Wågberg, L. Adsorption of Xyloglucan onto Cellulose Surfaces of Different Morphologies: An Entropy-Driven Process. *Biomacromolecules* **2016,** *17*(9), p2801. https://doi.org/10.1021/acs.biomac.6b00561.

(118) Jain, K.; Reid, M. S.; Larsson, P. A.; Wågberg, L. On the Interaction between PEDOT:PSS and Cellulose: Adsorption Mechanisms and Controlling Factors. *Carbohydr. Polym.* **2021**, *260,* p117818. https://doi.org/10.1016/j.carbpol.2021.117818.

(119) Katsir, Y.; Shapira, Y.; Mastai, Y.; Dimova, R.; Ben-Jacob, E. Entropic Effects and Slow Kinetics Revealed in Titrations of D 2O-H2O Solutions with Different D/H Ratios. *J. Phys. Chem. B* **2010**, *114* (17), p5755. https://doi.org/10.1021/jp909657m.

(120) Engdahl, A.; Nelander, B. On the Relative Stabilities of H- And D-Bonded Water Dimers. *J. Chem. Phys.* **1986**, *86* (4), p1819. https://doi.org/10.1063/1.452182.

(121) Soper, A. K.; Benmore, C. J. Quantum Differences between Heavy and Light Water. *Phys. Rev. Lett.* **2008**, *101* (6), p1. https://doi.org/10.1103/PhysRevLett.101.065502.

(122) Ozawa, T.; Asakawa, T.; Garamus, V. M.; Ohta, A.; Miyagishi, S. Effect of D2O Solvent on the Micellization Behaviour of 2-Hydroxy-1,1,2,3,3-Pentahydroperfluoroundecyldiethyl-Ammonium Halides. *J. Oleo Sci.* **2005**, *54* (11), p585. https://doi.org/10.5650/jos.54.585.

(123) Y M Efimova 1, S Haemers, B Wierczinski, W Norde, A. A. van W. Stability of Globular Proteins in H_2O and D_2O. *Biopolymers* **2007**, *85* (3), p264. https://doi.org/https://doi.org/10.1002/bip.20645.

(124) Giglio, A. Calcite Scale Formation in the Green Liquor Handling System of the Kraft Chemical Recovery Process , Diss. University of Toronto (Canada), **2018.**

(125) Das, N.;Bose, S.; Biswas, D. Effect of Magnesium-Salts on Hydrogen Peroxide Bleaching of Non-Wood Pulps. *Bangladesh J. Sci. Ind. Res.* **2016**, *51* (4), p291.

(126) Johannsmann, D.; Mathauer, K.; Wegner, G.; Knoll, W. Viscoelastic Properties of Thin Films Probed with a Quartz-Crystal Resonator. *Phys. Rev. B* **1992**, *46*, p7808. https://doi.org/10.1103/PhysRevB.46.7808.

(127) Ahmad, F. B.; Williams, P. A. Effect of Salts on the Gelatinization and Rheological Properties of Sago Starch. *J. Agric. Food Chem.* **1999**, *47*(8), 3359. https://doi.org/10.1021/jf981249r.

(128) Huynh, U. T. D.; Lerbret, A.; Neiers, F.; Chambin, O.; Assifaoui, A. Binding of Divalent Cations to Polygalacturonate: A Mechanism Driven by the Hydration Water. *J. Phys. Chem. B* **2016**, *120*(5), p1021 https://doi.org/10.1021/acs.jpcb.5b11010.

(129) Khanjani, P.; Kosonen, H.; Ristolainen, M.; Virtanen, P.; Vuorinen, T. Interaction of Divalent Cations with Carboxylate Group in TEMPO-Oxidized Microfibrillated Cellulose Systems. *Cellulose* **2019,** *26*, p4841. https://doi.org/10.1007/s10570-019-02417-w.

(130) Obiweluozor, F. O.; Ghavaminejad, A.; Hashmi, S.; Vatankhah-Varnoosfaderani, M.; Stadler, F. J. A NIPAM-Zwitterion Copolymer: Rheological Interpretation of the Specific Ion Effect on the LCST. *Macromol. Chem. Phys.* **2014**, *215*, p1077. https://doi.org/10.1002/macp.201300778.

(131) Hancock, R. D.; Marsicano, F. Parametric Correlation of Formation Constants in Aqueous Solution. 2. Ligands with Large Donor Atoms. *Inorg. Chem.* **1980**, *19*(9), p2709. https://doi.org/10.1021/ic50211a045.

(132) Thibault, J. F.; Rinaudo, M. Interactions of Mono- and Divalent Counterions with Alkali- and Enzyme-deesterified Pectins in Salt-free Solutions. *Biopolymers* **1985**, *24*(11), p2131. https://doi.org/10.1002/bip.360241109.

(133) Thom, D.; Grant, G. T.; Morris, E. R.; Rees, D. A. Characterisation of Cation Binding and Gelation of Polyuronates by Circular Dichroism. *Carbohydr. Res.* **1982**,*100*(1), p29. https://doi.org/10.1016/S0008-6215(00)81023-X.

(134) Mitroy, J.; Safronova, M. S.; Clark, C. W. Theory and Applications of Atomic and Ionic Polarizabilities. *Journal of Physics B: Atomic, Molecular and Optical Physics*. **2010**, *43*(20), p202001. https://doi.org/10.1088/0953-4075/43/20/202001.

(135) Ninham, B. W.; Lo Nostro, P. *Molecular Forces and Self Assembly:In Colloid, Nano Sciences and Biology*; **2010**. https://doi.org/10.1017/CBO9780511811531.

(136) Sharratt, W. N.; O'Connell, R.; Rogers, S. E.; Lopez, C. G.; Cabral, J. T. Conformation and Phase Behaviour of Sodium Carboxymethyl Cellulose in the Presence of Mono- And Divalent Salts. *Macromolecules* **2020**, *53* (4), p1451. https://doi.org/10.1021/acs.macromol.9b02228.

(137) Stetefeld, J.; McKenna, S. A.; Patel, T. R. Dynamic Light Scattering: A Practical Guide and Applications in Biomedical Sciences. *Biophys. Rev.* **2016**, *8* (4), p409. https://doi.org/10.1007/s12551-016-0218-6.

(138) Arumughan, V.; Nypelö, T.; Hasani, M.; Brelid, H.; Albertsson, S.; Wågberg, L. & Larsson, A. Specific Ion Effects in the Adsorption of Carboxymethyl Cellulose: The Influence of Industrially Relevant Divalent Cations. *Colloids Surfaces A ; Physicochem. Eng. Asp.* **2021**, *626*, p127006.

(139) Valencia, L.; Nomena, E. M.; Monti, S.; Rosas-Arbelaez, W.; Mathew, A. P.; Kumar, S.; Velikov, K. P. Multivalent Ion-Induced Re-Entrant Transition of Carboxylated Cellulose Nanofibrils and Its Influence on Nanomaterials' Properties. *Nanoscale* **2020**, *12* (29), p15652. https://doi.org/10.1039/d0nr02888f.

(140) Köhnke, T.; Östlund, Å.; Brelid, H. Adsorption of Arabinoxylan on Cellulosic Surfaces: Influence of Degree of Substitution and Substitution Pattern on Adsorption Characteristics. *Biomacromolecules* **2011**, *12* (7), p2633. https://doi.org/10.1021/bm200437m.

(141) Simonsson, I.; Sögaard, C.; Rambaran, M.; Abbas, Z. The Specific Co-Ion Effect on Gelling and Surface Charging of Silica Nanoparticles : Speculation or Reality ? *Colloids Surfaces A* **2018**, *559* , p334. https://doi.org/10.1016/j.colsurfa.2018.09.057.

(142) Robinson, J. B.; Strottmann, J. M.; Stellwagen, E. Prediction of Neutral Salt Elution Profiles for Affinity Chromatography. *Proc. Natl. Acad. Sci. U. S. A.* **1981**, *78* (4), p2287. https://doi.org/10.1073/pnas.78.4.2287.

(143) Smith, D. W. Ionic Enthalpies. *J. Chem. Educ.* **1977**, *1* (22), p1.

(144) Kocherbitov, V. The Nature of Nonfreezing Water in Carbohydrate Polymers. *Carbohydr. Polym.* **2016**, *150*, p353. https://doi.org/10.1016/j.carbpol.2016.04.119.

(145) Lindman, B.; Medronho, B.; Alves, L.; Norgren, M.; Nordenskiöld, L. Hydrophobic Interactions Control the Self-Assembly of DNA and Cellulose. *Q. Rev. Biophys.* **2021**, *54* (2016), p3. https://doi.org/10.1017/S0033583521000019.

(146) Schelero, N.; Hedicke, G.; Linse, P.; Klitzing, R. V. Effects of Counterions and Co-Ions on Foam Films Stabilized by Anionic Dodecyl Sulfate. *J. Phys. Chem. B* **2010**, *114* (47), p15523. https://doi.org/10.1021/jp1070488.

(147) Sett, S.; Karakashev, S. I.; Smoukov, S. K.; Yarin, A. L. Ion-Specific Effects in Foams. *Adv. Colloid Interface Sci.* **2015**, *225*, p98. https://doi.org/10.1016/j.cis.2015.08.007.

(148) Danov, K. D.; Basheva, E. S.; Kralchevsky, P. A. Effect of Ionic Correlations on the Surface Forces in Thin Liquid Films: Influence of Multivalent Coions and Extended Theory. *Materials (Basel).* **2016**, *9* (3), p145. https://doi.org/10.3390/ma9030145.

(149) Karakashev, S. I. *Hydrodynamics of Foams*; Springer Berlin Heidelberg, **2017**; *58* (8)p1. https://doi.org/10.1007/s00348-017-2332-z.

(150) Leontidis, E. Investigations of the Hofmeister Series and Other Specific Ion Effects Using Lipid Model Systems. *Adv. Colloid Interface Sci.* **2017**, *243*, p8. https://doi.org/10.1016/j.cis.2017.04.001.

(151) Xu, M.; Tang, C. Y.; Jubb, A. M.; Chen, X.; Allen, H. C. Nitrate Anions and Ion Pairing at the Air-Aqueous Interface. *J. Phys. Chem. C* **2009**, *113* (6), p2082. https://doi.org/10.1021/jp805376x.

Appendix

S1. Materials

The cellulose nanofibers (CNF) with an average diameter of 5 nm and carboxylic content of 31.4 µmol/g from softwood Kraft fibers were obtained from Stora Enso, Stockholm. The nanocellulose fibers have a residual hemicellulose content of 14.7% (xylose 8%, arabinose 0.62%, galactose 0.25%, and mannose 6.1%) and lignin content of 1.1% (Klason lignin 0.35% and acid-soluble lignin 0.75%). A never-dried Scandinavian softwood Kraft pulp from Södra Cell was used in the experiments with cellulose fibres. The pulp was industrially produced and had been bleached in an elemental chlorine-free (ECF) sequence, namely D(OP)D(PO), where D stands for a stage with the addition of chlorine dioxide, OP for an oxygen delignification stage and PO for a pressurized peroxide stage. This bleaching was performed until ISO Brightness 90% was reached. Magnesium chloride ($MgCl_2$), calcium chloride ($CaCl_2$), magnesium nitrate ($Mg(NO_3)_2$), magnesium bromide ($MgBr_2$), magnesium sulfate ($MgSO_4$), zinc sulfate ($ZnSO_4$), zinc nitrate ($Zn(NO_3)_2$), Deuterium oxide (D_2O) and polyethyleneimine-branched polymers (with an average Mw of 25 kDa) were purchased from Sigma Aldrich. Carboxymethylcellulose (Blanose 7LPEP) with a molecular weight of 90.5 kDa and a degree of substitution (DS) of 0.7 (according to the supplier) was kindly provided by Ashland.Ultra-filtrated (Mw>500 kD) poly-DADMAC (Mw 550 kD) with a charge density of 6.2 meq/g was purchased from RISE, Stockholm, and polyethylene sodium sulphonate (Na-PES) from Paper Test Equipment AB, Sweden. All polymers were used as received.

S2. Preparation and characterization of CNF thin film on QCM-D Sensor

The QCM-D sensors were cleaned by immersing them in a 10% NaOH solution for 20 seconds. The sensors were rinsed with water and then dried with nitrogen. After cleaning the sensor, UV-ozone treatment was done for 10 minutes. Then, it was immersed in 1.6 g/L PEI solution to form a positively charged anchoring layer. The spin coating solution was prepared by dispersing CNF in water (1.7 g/L) for 5 minutes using probe sonication (20 % power). After that, the dispersion was centrifuged for 40 minutes (6000 rpm). The supernatant solution was transferred into another vessel. This is the spin coating suspension.

The produced cellulose dispersion was then spin coated over a PEI-coated QCM-D surface for 1 minute using a spin coater (3000 rpm, acceleration of 2100 rpm/s). The films were then dried in a desiccator after being processed in an oven for 10 minutes at 80 °C.

The film morphology and uniformity were analyzed using atomic force microscopy (INTEGRA Prima setup NT-MDT Spectrum Instruments, Moscow, Russia). Three randomly chosen locations on the film were measured in semi-contact mode, and the root-mean-square roughness was determined using the Gwyddion software.

The water content of the CNF model film was determined using a QCM-D equipment in accordance with the procedure described by Kittle et al.[1]. (Biolin Scientific, Gothenburg, Sweden). The QCM-D sensors were put in the flow cell and deionized water was injected at a rate of 100 µL per minute for 3 hours to establish a stable baseline. Then the solvent was switched to D_2O, and the response was recorded until a plateau in the frequency shift occurred. After that, the solvent was switched back to H_2O again. Calculation of the water contained in the film was based on the advantage of the density difference of H_2O and D_2O.

S3. Preparation of fibres for the adsorption studies

It has previously been demonstrated that fines from cellulose fibers absorb significantly more polymers due to their greater specific surface area[2]. Fines were thus removed using a Dynamic Drainage Jar with a screening diameter of 76 µm and the resulting fines-free cellulose fibres were ion-exchanged into their sodium form according to the procedure described by Köhnke et al.[3].

S4. Adsorption of CMC on bleached softwood Kraft pulp fibres

Wet, pretreated cellulose-rich fibers weighing 5 g were dispersed in deionized water containing dissolved $CaCl_2$ or $MgCl_2$. The concentration of $CaCl_2$ or $MgCl_2$ in the water phase was 20 mM after the addition of wet fibres, and the temperature of the fibre suspension was kept at 40 °C in a vibrating water bath. A CMC solution containing 20 mM salt ($CaCl_2$ or $MgCl_2$) was added to the fiber suspension, and the pH was adjusted to 7 using 0.01 M sodium hydroxide. The ultimate consistency of the fiber suspension was 5% (w/w percent). After 2 hours, the suspension was filtered and washed with 750 ml of corresponding salt solution (20 mM); the first filtrate and washed pulp were separated for further analysis. The control studies were carried out in various salt settings without the addition of CMC but with the same other parameters, such as consistency, pH, and temperature, as previously.

S5. Analysis of the total charge of the modified pulp by conductometric titration

The total charge of the reference pulp and the CMC modified pulp under different salt environments was also analyzed by conductometric titration. The modified pulp was protonated by treating it with 0.1 M HCl solution and the pH was adjusted to 2. The protonated pulp was washed thoroughly to remove the excess

amount of acid before being titrated against 0.01 M NaOH using an automated conductometric titrator (Metrohm Conductivity Module 856, Sweden).

S6. Analysis of the surface charge of modified pulp by polyelectrolyte titration

Polyelectrolytic titration was used to determine the surface charge of the modified and and unmodified cellulose rich fibers[4]. The carboxylate groups in the pulp were ion-exchanged into their sodium form prior to titration. To begin, 5 g of pulp was protonated by immersing it in 0.01 M HCl (0.5 percent pulp consistency) and adjusted to a pH of 2 with a 0.1 M HCl solution. The pulp was then soaked for 30 minutes before being dewatered with a Büchner funnel and washed with deionized water until the conductivity of the filtrate was less than 5 µS/cm. The dewatered pulp was transferred to a beaker containing 1000 ml of 1 mM $NaHCO_3$, and the resulting pulp suspension was stirred before 0.1 M of NaOH was added to obtain a constant pH of 9. After 30 minutes, the pulp was dewatered with a Büchner funnel and rinsed with deionized water until the filtrate's conductivity was less than 5 µS/cm.

Five sections of the pulp were added to a mixture of 75 ml deionized water and 5 ml 0.2 mM NaCl, each equivalent to approximately 0.5 g (1/10 of the wet pulp in its sodium form). The diluted pulp samples were treated with five levels of a polyDADMAC solution (0.5 g/L), and the final volume of water in each sample was adjusted to 100 ml by adding deionized water. The samples were then agitated for 30 minutes before the pulp was dewatered using a Büchner funnel. The resultant pulp was dried and weighed to estimate the amount of pulp in each sample, and the filtrate was tested for non-adsorbed polyDADMAC by titration with 0.2 mM Na-PES using a Mütek PCD 03 apparatus. The adsorption isotherm was then used to compute the surface charge.

S7. Total organic carbon analysis and Anionic charge content using direct polyelectrolyte titration

• Following adsorption, the filtrates were subjected to Total Organic Carbon (TOC) measurement in accordance with SS-EN 1484 using a TOC 5050A Schimadzu analyzer to estimate the quantity of unabsorbed CMC contained in the filtrate.

• The anionic charge of the filtrate was determined using titration of the filtrate collected from the reference pulp and the CMC modified pulp in various salt conditions. The pulps were filtered via a Büchner funnel with a 100 µM nylon filter, and 10 mL of the filtrate was titrated with 0.2 mM PolyDADMAC using a Mütek PCD 03 apparatus (Germany).

Table A1. Total Organic Content (TOC) and anionic trash content of the filtrate left after the adsorption from $MgCl_2$ and $CaCl_2$.

Salt	Total Organic Content (TOC) mg/L			Anionic trash content (μeq/L)		
	CMC (0 g/kg)	CMC (5g/kg)	CMC (20 g/kg)	CMC (0 g/kg)	CMC (5 g/kg)	CMC (20 g/kg)
$MgCl_2$	3.00 ± 0.02	73.70 ± 0.02	350 ± 1	3.4 ± 0.1	825 ± 9	3756 ± 30
$CaCl_2$	2.00 ± 0.03	69.80 ± 0.02	343 ± 1.5	3.2 ± 0.1	786 ± 13	3676 ± 29

S8. Adsorption experiments using QCM-D

The adsorption behaviour of carboxymethyl celluloses onto model cellulose nanofibre films was monitored using QCM-D (Biolin Scientific, Gothenburg). In this thesis, the adsorption experiments have carried out in presence of different concentrations of salts. In general, CMC solutions of concentration 0.02% or 0.2% (w/v) containing a salt (ranging from 5 mM to 250 mM ionic strength in article 2 and article 3, a concentration range of 0.002 M to 0.02 M in article 4.) were injected into the flow cells. The frequency changes were registered at 5 MHz fundamental resonance frequency and its several overtones.

In temperature dependent adsorption studies, the buffer solution and the CMC solutions were degassed using a bath sonicator before the experiments to avoid bubble formation in the QCM-D cell. The solutions were preheated to the 45^0C prior to the injection to minimize the temperature variation in the cell.

The swelling-deswelling studies were carried out at a flow rate of flow rate of 20 μL/min. It is important that the flow rate be kept small to prevent flow-induced desorption. The adsorbed layers of CMC (from 20 mM of $CaCl_2$ and 20 mM NaCl) were subjected to swelling by introducing distilled water into the flow cell. The swollen CMC layers were subjected to deswelling by the introduction of corresponding salt solution into the flow cell.

The data obtained from QCM-D experiments were then exported to excel format using Qtools software, analysed and plotted using Origin software.

S9. Isothermal titration calorimetry experiments

An isothermal titration calorimeter (VP-ITC microcalorimeter from GE Healthcare) was used to determine the enthalpies for the binding of carboxymethyl cellulose to cellulose nanofiber suspension at 25 °C. Before each experiment, all solutions were degassed for 15 min. A solution of CMC (2 g/L) containing 10 mM NaCl was added sequentially to 1.46 mL titration cell initially containing 0.5 g/L of CNF solution at 10 mM NaCl. 28 injections of 5 μL were done and heat changes were recorded.

Reference

(A1) Kittle, J. D.; Du, X.; Jiang, F.; Qian, C.; Heinze, T.; Roman, M.; Esker, A. R. Equilibrium Water Contents of Cellulose Films Determined via Solvent Exchange and Quartz Crystal Microbalance with Dissipation Monitoring. Biomacromolecules 2011, *12*(8), p2881. https://doi.org/10.1021/bm200352q.

(A2) Wågberg, L.; Bjorklund, M. Adsorption of Cationic Potato Starch on Cellulosic Fibres. *Nord. Pulp Pap. Res. J.* **2007**, *8(*4), p399 https://doi.org/10.3183/npprj-1993-08-04-p399-404.

(A3) Köhnke, T.; Brelid, H.; Westman, G. Adsorption of Cationized Barley Husk Xylan on Kraft Pulp Fibres: Influence of Degree of Cationization on Adsorption Characteristics. *Cellulose* **2009**, *16*(6), p1109 https://doi.org/10.1007/s10570-009-9341-x.

(A4) Horvath, A. E. The Effects of Cellulosic Fibre Charges on Polyelectrolyte Adsorption and Fibre-Fibre Interactions, KTH, **2006**.